Mitochondrial and Chloroplast Stress Responses Are Modulated in Distinct Touch and Chemical Inhibition Phases[1][OPEN]

Olivier Van Aken*, Inge De Clercq, Aneta Ivanova, Simon R. Law, Frank Van Breusegem, A. Harvey Millar, and James Whelan

ARC Centre of Excellence in Plant Energy Biology, Faculty of Science, The University of Western Australia, Crawley 6009, Western Australia, Australia (O.V.A., A.I., A.H.M.); Department of Botany, ARC Centre of Excellence in Plant Energy Biology, School of Life Science, La Trobe University, Melbourne, Victoria 3086, Australia (I.D.C., S.R.L.); Department of Plant Systems Biology, VIB, Ghent University, B-9052 Gent, Belgium (I.D.C., F.V.B.); Department of Plant Biotechnology and Bioinformatics, Ghent University, B-9052 Gent, Belgium (I.D.C., F.V.B.); and Department of Plant Physiology, Umeå Plant Science Centre, Umeå University, S-90187 Umeå, Sweden (S.R.L.)

ORCID IDs: 0000-0003-4024-968X (O.V.A.); 0000-0001-8125-1239 (I.D.C.); 0000-0003-0389-6650 (S.R.L.); 0000-0002-3147-0860 (F.V.B.).

Previous studies have identified a range of transcription factors that modulate retrograde regulation of mitochondrial and chloroplast functions in Arabidopsis (*Arabidopsis thaliana*). However, the relative importance of these regulators and whether they act downstream of separate or overlapping signaling cascades is still unclear. Here, we demonstrate that multiple stress-related signaling pathways, with distinct kinetic signatures, converge on overlapping gene sets involved in energy organelle function. The transcription factor ANAC017 is almost solely responsible for transcript induction of marker genes around 3 to 6 h after chemical inhibition of organelle function and is a key regulator of mitochondrial and specific types of chloroplast retrograde signaling. However, an independent and highly transient gene expression phase, initiated within 10 to 30 min after treatment, also targets energy organelle functions, and is related to touch and wounding responses. Metabolite analysis demonstrates that this early response is concurrent with rapid changes in tricarboxylic acid cycle intermediates and large changes in transcript abundance of genes encoding mitochondrial dicarboxylate carrier proteins. It was further demonstrated that transcription factors *AtWRKY15* and *AtWRKY40* have repressive regulatory roles in this touch-responsive gene expression. Together, our results show that several regulatory systems can independently affect energy organelle function in response to stress, providing different means to exert operational control.

As plants are sessile organisms, they must respond in an energy-efficient and effective way to cope with continuous change in the environment. Chloroplasts provide the energy equivalents to reduce CO_2 to carbohydrates via photosynthesis. Plant mitochondria are crucial to support energy metabolism, photosynthetic and photorespiratory functions, survival during dark periods, and meristem activity (Ishizaki et al., 2006; Van Aken et al., 2007; Howell et al., 2009; Araújo et al., 2014). As mitochondria and chloroplasts are tightly involved in cellular metabolism, they are in a prime position to sense cellular dysfunction and are therefore thought to be one of the initial sites of stress recognition and can contribute to programmed cell death execution (Vanlerberghe, 2013). A significant body of evidence supports a crucial role for mitochondria and chloroplasts in perceiving and responding to biotic and abiotic stress conditions (Skirycz et al., 2010; Leister et al., 2011; Nomura et al., 2012; Zhang et al., 2014; Stael et al., 2015). This is further supported by several studies demonstrating that the transcriptomic response to mitochondrial or chloroplast dysfunction by chemical or genetic disruption appears to be part of broad biotic and abiotic stress responses (Schwarzländer et al., 2012; Van Aken and Whelan, 2012).

For mitochondria and chloroplasts to be involved in this cellular signaling network, communication from nucleus to organelle (anterograde) and from organelle to nucleus (retrograde) is essential (Ng et al., 2014). In terms of anterograde signals, it is known that nuclear genes encoding mitochondrial proteins respond to the diurnal cycle (Giraud et al., 2010), sugar content (Comelli et al., 2012), stress conditions (Van Aken et al., 2009), and germination cues (Law et al., 2012). On the other hand, retrograde signaling has been studied extensively by using chemical inhibition of organellar function (e.g. antimycin A, methyl viologen, and norflurazon). Several studies showed that a subset of nuclear genes consistently responds to inhibition of mitochondrial function (Van Aken et al., 2007; Schwarzländer et al., 2012; De Clercq et al., 2013). This group of genes was termed the mitochondrial dysfunction stimulon (De Clercq et al., 2013) and contains several genes that play important roles in stress tolerance in Arabidopsis (*Arabidopsis thaliana*). For example, the glycosyltransferase UGT74E2 targets auxins and

upon overexpression triggers profuse shoot branching and drought tolerance (Tognetti et al., 2010). Also, the classical mitochondrial stress marker gene alternative oxidase *AOX1a* was found to be important during osmotic stress (Dojcinovic et al., 2005; Dahal et al., 2014), and recently it was shown that the mitochondrial outer membrane ATPase AtOM66 (AtBCS1) is a regulator of cell death that controls pathogen resistance, senescence, and drought tolerance (Zhang et al., 2014). Therefore, it is evident that energy organelle signaling is an important part of general stress responses, and understanding the way it is controlled could provide a means to enhance stress tolerance and, thus, productivity in crop species.

Over the past few years, regulatory proteins that are involved in retrograde responses in plants have been identified. Using a reverse genetic approach, a number of transcription factors were identified, such as ABI4 (Koussevitzky et al., 2007; Giraud et al., 2009), AtWRKY15, and AtWRKY40 (Shang et al., 2010; Vanderauwera et al., 2012; Van Aken et al., 2013). In a forward genetic screen using the *AOX1a* promoter fused to luciferase, several genes that influenced plant retrograde signaling were identified. A cyclin-dependent kinase, CDKE;1, was found as a positive regulator of both mitochondrial retrograde signaling and chloroplast signaling (Ng et al., 2013a; Blanco et al., 2014). Additionally, a group of transmembrane NAC-type transcription factors was identified and shown to positively regulate mitochondrial retrograde signaling (De Clercq et al., 2013; Ng et al., 2013b) by binding a mitochondrial dysfunction DNA motif. Surprisingly, subcellular localization studies showed that some of these NAC transcription factors are anchored in the endoplasmic reticulum (ER) by their transmembrane domain. This suggests that the NAC transcription factors are released from the ER upon stress perception and subsequently translocate to the nucleus. Furthermore, application of rhomboid protease inhibitors was able to partially suppress retrograde induction, indicating NAC transcription factors are released by proteolytic cleavage (Ng et al., 2013b). Inhibitors targeting ER and mitochondrial Ca^{2+} channels were demonstrated to enhance or reduce stress responsiveness of MDR genes (Vanderauwera et al., 2012), further pointing toward a role for the ER. It was also found that an antagonistic relationship occurs between retrograde and auxin signaling. Loss of transporters involved in auxin distribution such as PIN1 and BIG results in an enhanced activation of mitochondrial retrograde response upon stimulation, while exogenous application of auxin suppresses retrograde signaling (Ivanova et al., 2014; Kerchev et al., 2014).

The relative importance of these regulators and whether they act downstream of separate or overlapping signaling cascades feeding into expression of common genes is still unclear. Here, we demonstrate that multiple stress-related signaling pathways, with distinct time signatures, converge on overlapping gene sets involved in chloroplast and mitochondrial function. When plants are spray-treated with mitochondrial or chloroplast inhibitors, one expression phase related to inhibitory activity of the active compound peaks around 3 to 6 h after treatment and is largely controlled by ANAC017. Furthermore, a rapid phase of gene expression within 10 min of treatment also affects stress signaling target genes and correlates with rapid changes in metabolic substrate concentrations. We further demonstrate that this rapid phase is related to "touch" signaling and is modulated by WRKY transcription factors.

RESULTS

NAC Transcription Factors Involved in Mitochondrial Retrograde Signaling Show Divergent Expression Patterns

Two previous studies identified five membrane-anchored NAC transcription factors as transcriptional regulators of plant mitochondrial retrograde signaling (De Clercq et al., 2013; Ng et al., 2013b), so the first aim was to clarify their relative contributions to retrograde signaling. To do this, we assessed transcript abundance of NACs in 2-week-old seedlings treated with monofluoroacetate (MFA; a tricarboxylic acid [TCA] cycle inhibitor) for 6 h (Fig. 1). *ANAC017* transcripts were most highly abundant in both untreated and stressed conditions, but showed no significant stress induction. Its closest homolog, *ANAC016*, was almost 1,300 times less abundant and was not further characterized in this study. *ANAC013* was highly inducible, but even after induction transcript levels were still less abundant than *ANAC017* in untreated conditions. Similar induction patterns were observed for *ANAC053*

[1] This work was supported by the facilities of the Australian Research Council Centre of Excellence Program (CE140100008). O.V.A. was supported by an Australian Research Council APD fellowship and grant (DP110102868 and DP160103573) and A.H.M. by an ARC Future Fellowship and ARC grant (FT110100242; DP130102918; and DP160103573). I.D.C. holds a postdoctoral fellowship from Research Foundation-Flanders (FWO-Vlaanderen FWO/PDO14/043) and is also supported by FWO travel grant 12N2415N. F.V.B. was supported by grants from the Interuniversity Attraction Poles Programme (IUAP P7/29 'MARS') initiated by the Belgian Science Policy Office and Ghent University (Multidisciplinary Research Partnership 'Biotechnology for a Sustainable Economy'; grant 01MRB510W).

* Address correspondence to olivier.van.aken@uwa.edu.au.

The author responsible for distribution of materials integral to the findings presented in this article in accordance with the policy described in the Instructions for Authors (www.plantphysiol.org) is: Olivier Van Aken (olivier.van.aken@uwa.edu.au).

O.V.A., J.W., A.H.M., F.V.B., and I.D.C. designed experiments; O.V.A. performed all experiments and data analysis; I.D.C. isolated and genotyped *anac053* and *anac078* knockout lines; I.D.C. and O.V.A. cloned and created promoter-GUS reporter lines for *ANAC017*, *ANAC053*, and *ANAC078*, overexpression lines for *ANAC017*, and cloned ANAC053 and ANAC078 GFP vectors; A.I. optimized qRT-PCR assays for *ANAC* quantitation; O.V.A. and A.H.M. wrote the manuscript in collaboration with all co-authors.

[OPEN] Articles can be viewed without a subscription.

www.plantphysiol.org/cgi/doi/10.1104/pp.16.00273

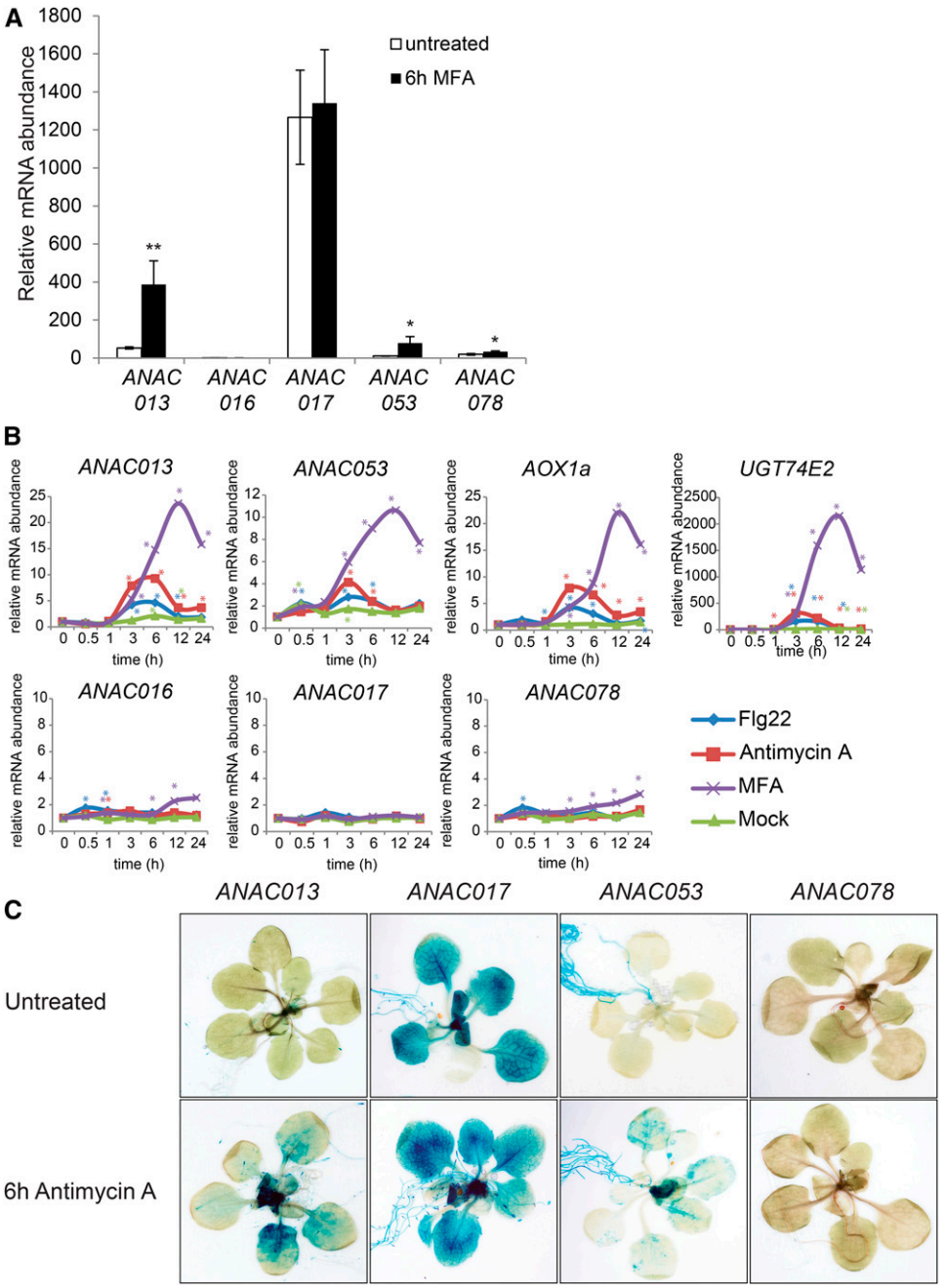

Figure 1. Expression of NAC transmembrane transcription factors. A, mRNA abundance of NAC transcription factors was quantified using qRT-PCR in 2-week-old in vitro-grown pooled Arabidopsis seedlings, before treatment and 6 h after treatment with 50 μM MFA (n = 3; mean ± SE). Expression levels were normalized to *ANAC016* expression in untreated conditions (set to 1). Asterisk indicates significant induction of mRNA levels after MFA treatment compared to untreated control ($P < 0.05$). B, Two-week old in vitro-grown seedlings were spray treated with Flg22, antimycin A, MFA, or mock solution (water + Tween). Pooled plants were collected, and mRNA levels were measured by qRT-PCR (± SE) and normalized to untreated samples (0 h). *$P < 0.05$ versus 0 h ($n = 3$). C, Promoter-GUS analysis of NAC expression patterns. The 1.5-kb promoter regions of selected NAC transcription factors fused to a GUS reporter gene were stably transformed into Arabidopsis Col-0 plants. Three-week-old in vitro-grown plants were stained for GUS activity before and after 6 h of treatment with 50 μM antimycin A.

and *ANAC078*: Both were significantly induced by MFA, but did not reach the high transcript abundance of *ANAC017*.

Next, detailed time-course experiments were performed with a wider range of stress-inducing factors: bacterial elicitor Flg22 and UV and chemical inhibitors operating on complex III (antimycin A) and the TCA cycle (MFA) were applied or sprayed on 2-week-old seedlings, along with a mock spray treatment control. Samples were collected at a range of time points over 24 h, and mRNA abundance of the transcription factors and their previously identified target genes *AOX1a* and *UGT74E2* were measured (Fig. 1B). In accordance with the previous MFA experiment, *ANAC016*, *ANAC017*, and *ANAC078* displayed no or very mild stress response. *ANAC013*, *ANAC053*, and the target genes *AOX1a* and *UGT74E2* showed a clear induction after 3 h of treatment. Transcript levels steadily decreased to almost basal levels 12 and 24 h after treatment, except for the MFA treatment, which provoked longer term induction. UV treatment caused the most gradual rates of induction over time and in some cases expression increased at 1 h (Supplemental Fig. S1).

To assess promoter activities, 3-week-old *GUS*-based reporter lines were sprayed with antimycin A (Fig. 1C). In untreated conditions the promoter of *ANAC017*

showed by far the strongest activity throughout the entire root and shoot of the plants, but in accordance with its transcript levels no obvious changes after stress treatment were observed (a magnified image of *ANAC017:GUS* activity in root tips is shown in Supplemental Fig. S1B). The promoter of *ANAC013* showed low but discernible expression in young leaves and root tips. After stress treatment, a clear induction in the leaves was observed, particularly in the youngest leaves, in line with a previous report (De Clercq et al., 2013). *ANAC053* showed clear promoter activity throughout the root, but expression in leaf tissues was only observed after stress treatment. *ANAC078* showed the weakest expression with some GUS staining in root tips, but no response to the stress treatment. Overall, these experiments show that *ANAC017* is the most strongly expressed but was not induced by stress treatments.

ANAC017 Is a Key Regulator of Responses to Chemical Mitochondrial Inhibition

To determine the effect of antimycin A treatment on the respiratory capacity of plants, dark respiration measurements were performed and showed no gross depletion of oxygen consumption after 4 h of antimycin A treatment compared to untreated controls (Supplemental Fig. S2B; $P > 0.50$, $n = 4$). This indicates that spray treatment with 50 μM antimycin A, while known to lead to cytochrome pathway inhibition and induction of AOX (Vanlerberghe and McIntosh, 1992; Ng et al., 2013b), is not a lethal chemical treatment, does not stop plant respiratory metabolism, and thus represents a reasonable model for assessing signaling responses following a partial mitochondrial dysfunction.

Next, to assess the individual contributions of previously identified transcription factors in plant retrograde signaling (belonging to NAC and WRKY families, and ABI4), we collected a set of unpublished and previously published loss- and gain-of-function mutants (see "Materials and Methods"). This set of 15 lines including the wild type (Col-0) was subjected to antimycin A treatment. Samples were collected at 0, 0.5, 1, 3, 6, and 12 h after treatment in three independent pools of approximately 20 2-week-old seedlings per genotype to account for individual variations. Transcript abundance of target genes was measured using qRT-PCR (Fig. 2). In untreated conditions, overexpression lines of *ANAC013*, *ANAC017*, *ANAC053*, and *ANAC078* already showed significantly elevated expression of *AOX1a* ($P < 0.05$) compared to Col-0 (Fig. 2, *AOX1a*, left panel, time 0). *ANAC013* itself was significantly ($P < 0.05$) induced in *ANAC017*, *ANAC078*, and *ANAC013* overexpression lines (Fig. 2; Supplemental Fig. S2, ANAC013 panels). *ANAC053* was significantly induced in *ANAC017* and *ANAC053* overexpression lines ($P < 0.05$; (Fig. 2, ANAC053 panels; Supplemental Fig. S2). Overall, these data suggest that all four NAC transcription factors upon overexpression have a basic capability of inducing mitochondrial retrograde signaling marker genes and some of its coregulators.

By far the most drastic effect was observed in *anac017* loss-of-function plants, where at the 3 h time point no significant induction of *AOX1a* (1.71-fold, $P = 0.47$) was observed compared to Col-0 0 h, as opposed to 10.4-fold induction in Col-0 ($P < 0.01$; Fig. 2). *anac017* loss-of-function lines also showed no induction of *ANAC013* and *ANAC053* at the 3 h time point, as opposed to 7.3-fold (*ANAC013*) and 2.9-fold (*ANAC053*) in Col-0 ($P < 0.05$). This indicates that *ANAC013* and *ANAC053* are target genes downstream of ANAC017 in the signaling cascade, further supported by the observation that *ANAC013* and *ANAC053* are constitutively induced in *ANAC017* overexpression plants (Fig. 2). At 6 h in *anac017*, only a mild induction of *AOX1a* and *ANAC013* was observed, which was significantly lower than in Col-0 ($P < 0.05$). None of the loss- or gain-of-function lines for other NAC, WRKY, or ABI4 transcription factors showed similarly strong reductions in antimycin A-induced target gene expression. In line with previous reports of ABI4 being a repressor of *AOX1a* expression, an increased expression of *AOX1a* was observed in *abi4-1* at the 0 h time point ($P < 0.05$; Giraud et al., 2009).

To confirm the robust nature of the upstream signaling role of ANAC017 in antimycin A-induced gene expression, a repeat experiment was performed on plants grown in soil and Col-0 was also compared to two independent *anac017* alleles (Supplemental Fig. S2C). In agreement, both *anac017* lines showed 4- to 6.5-fold reductions in *AOX1a* transcript induction at 3 h ($P < 0.01$, $n = 3$). At 6 h, *AOX1a* transcript levels were already falling in the Col-0 plants, but showed a delayed increase in the *anac017* lines that was well below the *AOX1a* levels reached in Col-0. Overall, these results indicate that ANAC017 is a key regulator of the transcriptional stress response to mitochondrial inhibition in seedlings grown in both Murashige and Skoog (MS) media and soil, and it is also regulating induction of *ANAC013* and *ANAC053.*

ANAC017 Affects Plant Resistance to Energy Organelle Inhibition

To consolidate that the role of ANAC017 extends beyond transcriptional responses, we performed a comprehensive phenotype analysis of all 15 NAC, WRKY, and ABI4 lines for resistance to constitutive energy organelle function inhibition (Fig. 3). To do this, the different plant lines were incubated on vertically positioned plates supplemented with antimycin A (complex III inhibitor), rotenone (complex I inhibitor), and methyl viologen (MV; a superoxide generator that leads to damage in chloroplasts in lighted conditions). Plants were grown for 7 d and primary root length was measured (Fig. 3). On control plates, a number of lines showed mild but significant growth reductions of between 13 and 30% compared to Col-0 plants. Antimycin A treatment resulted in significant growth reduction in

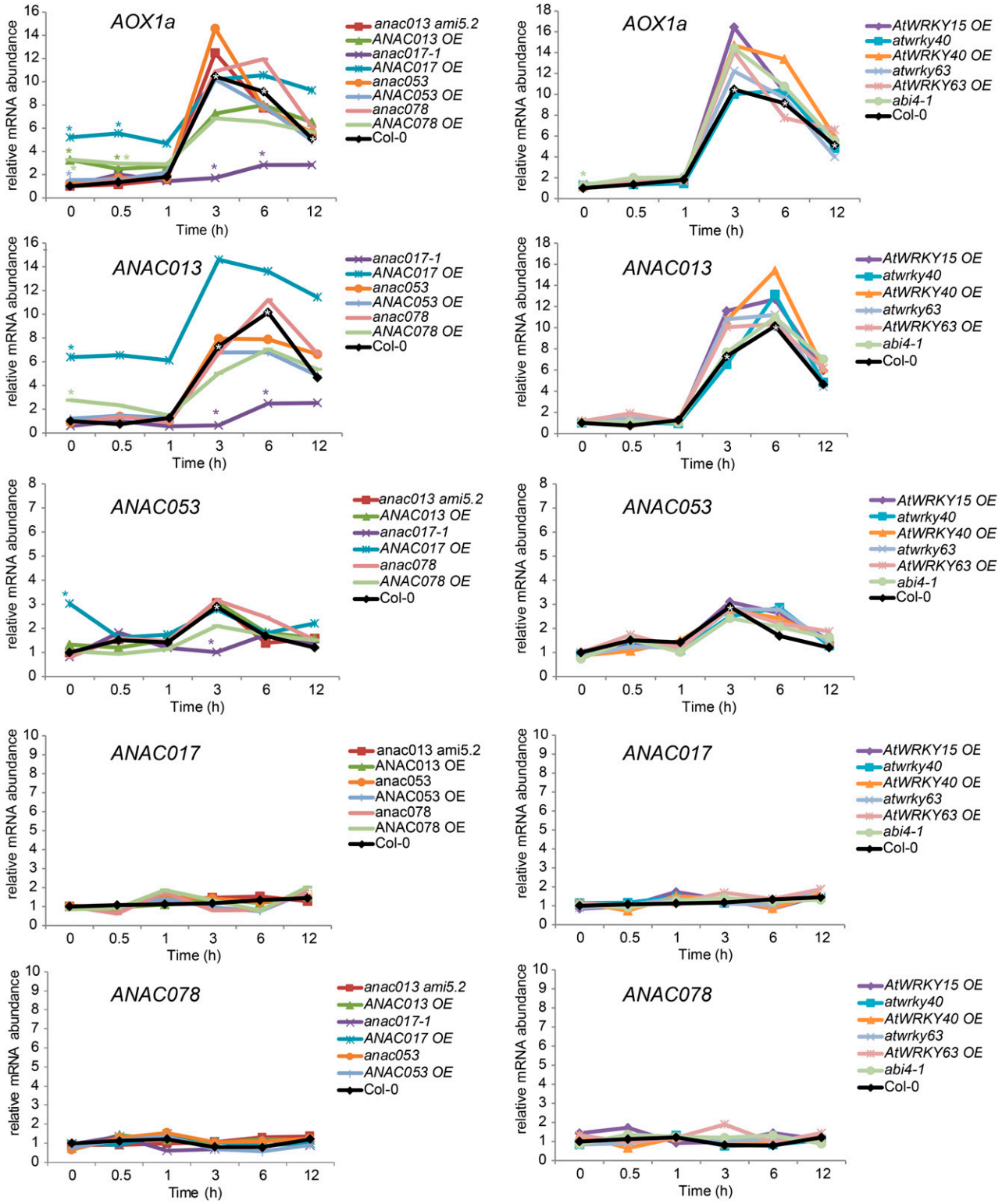

Figure 2. ANAC017 is a key regulator of antimycin A-induced mitochondrial retrograde signaling. Two-week-old in vitro-grown seedlings were spray treated with antimycin A. Plants were collected in pools, and relative mRNA levels were measured by qRT-PCR and normalized to Col-0 untreated samples (0 h). For clarity, *ANAC* transcript levels in their respective overexpression and loss-of-function lines were not displayed. Colored asterisks indicate statistically significant differential expression in a specific genotype versus Col-0 at the marked time point ($P < 0.05$; $n = 3$); white asterisks indicate statistically significant differential expression in Col-0 at the marked time point versus Col-0 0 h ($P < 0.05$; $n = 3$).

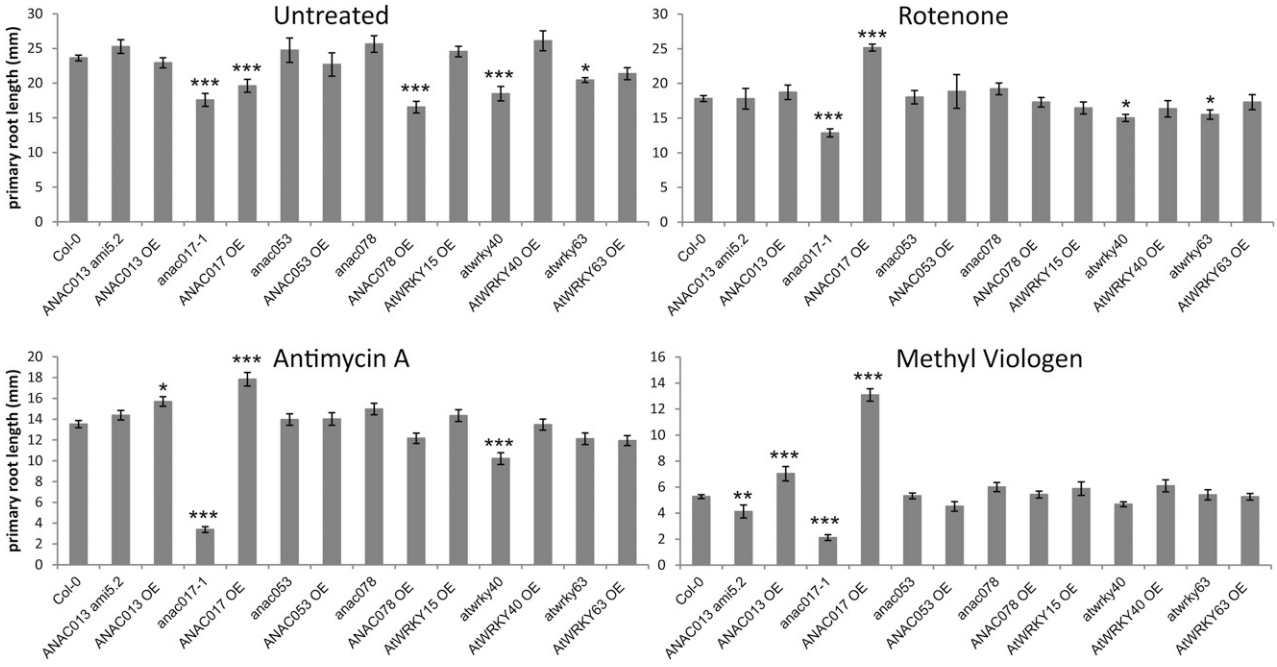

Figure 3. ANAC017 is a determinant of organelle dysfunction tolerance. Seeds of different genotypes were grown vertically on MS media plates supplemented with antimycin A, rotenone, or MV. Primary root growth was measured after 7 d in the growth chamber (±SE). Significant differences with Col-0 within the same treatment are indicated ($n > 7$, $^{*}P < 0.05$, $^{**}P < 0.01$, and $^{***}P < 0.001$).

all lines; *anac017* plants were particularly highly sensitive. In contrast, *ANAC017*- and *ANAC013*-overexpressing lines were significantly more tolerant to high concentrations of antimycin A. Rotenone had a milder effect on root length than antimycin A, but again plants overexpressing *ANAC017* showed significantly higher resistance than Col-0, while *anac017* plants were most susceptible. MV caused the most severe growth reductions (Fig. 3). Again, plants overexpressing *ANAC017* and *ANAC013* showed a significant resistance to MV compared to Col-0, while the *anac017* and *anac013* loss-of-function lines showed increased susceptibility. On the other hand, AtWRKY15, 40, 63, and ABI4 have no discernible effects specific to any of the treatments. From these results, it is apparent that ANAC017 is crucial for optimal plant growth under conditions of organellar inhibition and to a lesser extent also ANAC013 as reported previously (De Clercq et al., 2013).

ANAC017 Is Also a Regulator of Chloroplast Retrograde Signaling

Root growth characteristics showed a clear role for ANAC017 in resistance to antimycin A and rotenone. Interestingly, MV caused similar phenotypes in the gain- and loss-of-function lines of ANAC017 (Fig. 3). MV is generally considered as a photosynthesis inhibitor that accepts electrons directly from thylakoid photosystem I (Fd subunit) and transfers them to molecular oxygen generating superoxide. In light conditions, MV is regarded as a chloroplast-specific ROS generator (Tsang et al., 1991). We sprayed 2-week-old Col-0 and *anac017* seedlings with MV and assessed the effects on gene expression (Fig. 4). To confirm that MV did not cause a significant mitochondrial defect, the expression of mitochondrial dysfunction marker genes *AOX1a* and *AtOM66* was measured. The mock spray treatment caused mild inductions of both genes; however, no additional inductions were caused by the MV treatment (Fig. 4). It was also evident that ANAC017 is required for the mock induction at around 3 h. Based on an analysis of public microarray data, multiple marker genes were selected that respond more to MV treatment than mock (Kilian et al., 2007; Yoshida and Noguchi, 2009). qRT-PCR analysis revealed very high induction by MV of *HSP17.6A* (~80-fold) and *HSP17.6CII* (~250-fold) in Col-0, whereas no or minor inductions were caused in the mock treatment (Fig. 4). Other genes such as the *TINY* AP2 transcription factor, *sHSP23.5*, *AtWRKY30*, and *AtWRKY33* also showed severalfold higher induction in MV treatment compared to mock in Col-0. In contrast, the MV-inducible genes were up to 10-fold less induced in *anac017* plants compared to Col-0 (Fig. 4). These experiments indicate that ANAC017 is also involved in the transcriptional response that is triggered by chloroplast-generated superoxide signaling in response to MV.

The further assess the role of ANAC017 in chloroplast retrograde signaling, Col-0 and *anac017* plants were exposed to high light conditions (750 μmol s^{-1} m^{-2}). Samples were collected in biological triplicate and marker

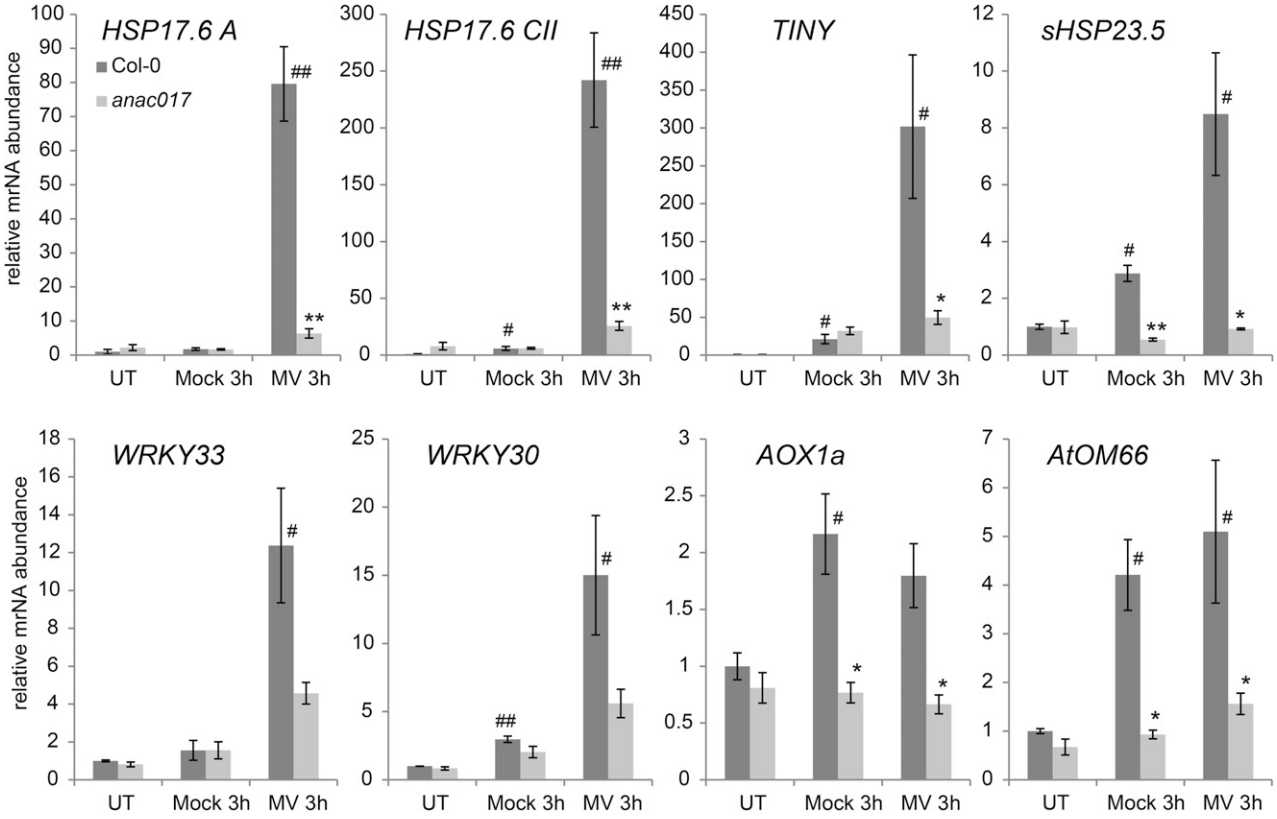

Figure 4. ANAC017 is a regulator of chloroplast stress response induced by MV. Two-week-old Col-0 and *anac017* plants were spray treated with mock solution or 50 μM MV. Pools of plants (n = 3) were collected in triplicate, and mRNA levels were measured by qRT-PCR (±SE). Statistically significant changes in Col-0 caused by treatments are indicated (#$P < 0.05$; ##$P < 0.01$). Statistically significant changes of *anac017* versus Col-0 within the same treatment are indicated (*$P < 0.05$; **$P < 0.01$).

genes were tested using qRT-PCR (Supplemental Fig. S3). *HSP17.6 A* and *HSP17.6 CII* were highly induced (>1,000-fold) by 1 h of high light in Col-0, while *AtAPX2* was induced ~150-fold. To determine if the transcripts responded to temperature changes caused by the high light treatment or the light itself, an additional control experiment was performed where plants were incubated under normal light conditions but at a temperature matching that observed in the plates during high light treatment (28°C). From this it was clear that exposure to high light, rather than elevated temperature, was the main contributor to the gene expression increases observed. Mitochondrial stress marker gene *AOX1a* showed mild but significant high light induction (3-fold). Overall, *anac017* plants showed no significant differences in high light-induced gene expression compared to Col-0 for any of the marker genes tested, indicating that ANAC017 plays no significant role in high light-induced signaling from the chloroplasts.

To clarify if ANAC017 plays a role in the previously described *GUN* (*genomes uncoupled*) pathway of chloroplast retrograde signaling (Susek et al., 1993), Col-0 and *anac017* plants were treated with the carotenoid biosynthesis inhibitor norflurazon, and the expression of GUN marker genes *LHCB1.1* and *LHCB2.4* was monitored (Supplemental Fig. S3B). As expected, transcript levels of *LHCB2.4* and *LHCB1.1* were strongly repressed within 3 h of norflurazon application, but no genotype-specific differences between Col-0 and *anac017* plants were found.

Stress Treatment by Spray Application Induces a Two-Phase Response in AtOM66 and WRKY Transcription Factors

The above experiments showed a clear role for NAC transcription factors, especially ANAC017, in retrograde responses to inhibitors around 3 h after treatment. Previous studies also identified *AtOM66* (encoding an outer mitochondrial membrane AAA ATPase) as a target for mitochondrial and chloroplast retrograde signaling but suggested it may be regulated differently to mitochondrial dysfunction stimulon genes such as *AOX1a* and *UGT74E2* (Ho et al., 2008; Van Aken and Whelan, 2012). As *AtOM66* was previously shown to be regulated by WRKY transcription factors via direct binding of the *AtOM66* promoter (Van Aken et al., 2013), stress-related (antimycin A, MFA, Flg22, and UV) WRKY expression patterns were examined by qRT-PCR as described in

Figure 1B (Fig. 5; Supplemental Fig. S1). AtWRKY63 showed an expression pattern very similar to *AOX1a* and *ANAC013* with stress-inducible expression peaking around 3 to 6 h after treatment for Flg22 and antimycin A and 12 h for MFA. Surprisingly, a more complex expression pattern was observed for *AtWRKY40*, *AtWRKY15*, and *AtOM66*, with a very high level of induction by the 30 min time point (>380-fold for *AtWRKY40*, >100-fold for *AtOM66*, and >10-fold for *AtWRKY15*), which rapidly declined by 1 h after treatment. Following this initial transient peak, these genes showed a second phase of induction similar in timing to *AOX1a* (Figs. 1B and 5). The mock treatment triggered a similar induction of the first peak, but showed much weaker induction than the inhibitors around 3 to 6 h. This indicates that the spray treatment itself appears to be the main cause for the first peak, while the stress-inducing active compounds are mostly responsible for the second phase for both NAC and WRKY transcription factors. To determine the effect of Tween 20 on the early response, a repeat experiment using water without Tween 20 for the spray treatment was performed, and this showed similar highly significant inductions within 25 min (e.g. AtWRKY40 was induced 226-fold, $P < 0.001$; Supplemental Fig, S4). In conclusion, *AtOM66* and its regulators *AtWRK40* and *AtWRKY15* display a two-phase expression pattern, with a rapid peak at 30 min caused by the physical spray treatment

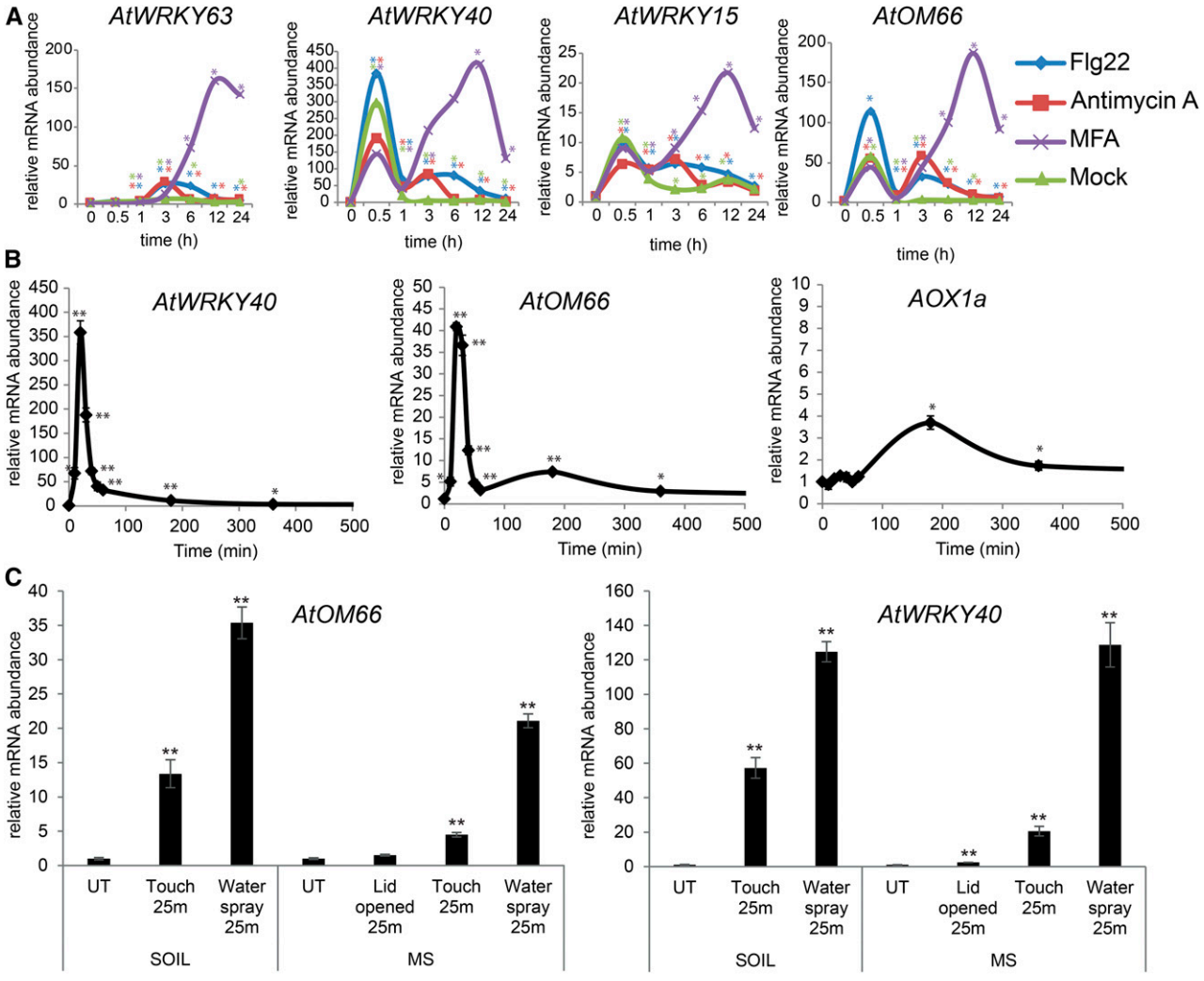

Figure 5. Spray treatment causes a two-phase stress response. A, Two-week-old in vitro-grown seedlings were spray treated with Flg22, antimycin A, MFA, or mock solution. Pooled plants were collected, and mRNA levels were measured by qRT-PCR and normalized to untreated samples (0 h). *$P < 0.05$ versus 0 h ($n = 3$). B, Two-week-old Col-0 plants were sprayed with water + Tween (mock), and pools of plants were collected in triplicate. mRNA levels were measured using qRT-PCR (mean ± SE) and normalized to time point 0 h. C, Two-week-old in vitro or soil-grown seedlings were treated as indicated. Pools of plants were collected ($n = 3$), and mRNA levels were measured by qRT-PCR and normalized to untreated samples (0 h). Statistically significant changes compared to untreated samples at time 0 h are indicated (*$P < 0.05$; **$P < 0.01$).

and a second peak around 3 h or later caused by the sprayed compound.

The Rapid Response Peak Is Related to Touch and Wounding Responses

To investigate this 30 min peak in more detail, a mock treatment time course was performed and samples were collected every 10 min during the first hour, then at 3, 6, and 24 h in triplicate pools (Fig. 5B). Significant induction of *AtOM66* (5.1-fold; $P < 0.02$) and *AtWRKY40* (67-fold; $P < 0.005$) was already observable by 10 min, with the highest expression level reached in the 20 to 30 min time points. *AOX1a* showed no significant induction at these early time points. Both *AtOM66* and *AOX1a* showed a mild but significant induction at the 3 h time point, possibly linked to the increased humidity and wetness caused by the spray treatment.

The rapid and highly transient nature of this early response could be caused by a number of different factors, including the mechanical stimulation of the spray treatment (similar to touch responses; Braam and Davis, 1990) or the changes in humidity and air composition by opening the petri dish plates. To investigate this, the effect of opening plates and mechanical stimulation by touching with blunt tweezers were each compared with the water spray treatment and a negative control. A similar control experiment was also performed on soil-grown plants. Samples of pooled plants were collected in triplicate after 25 min and mRNA expression levels of *AtOM66* and *AtWRKY40* were measured by qRT-PCR (Fig. 5C). The touch and water spray treatments caused rapid and strong inductions both in soil and in vitro, while just transiently opening the lid that led to minor vibrations resulted in minor inductions. The water spray was the most uniform manipulation of the leaf surfaces of the plants and gave the highest fold changes overall.

A number of previous studies have looked at touch and early wounding responses using genome-wide expression studies. In the Affymetrix ATH1 data set E-GEOD-48676, 5-week-old Arabidopsis leaves were wounded and collected 10 min after treatment. Although raw data files are publicly available on ArrayExpress, we could not find a published analysis. Therefore, we analyzed the data in detail. In total, 1127 probe sets of 22810 were significantly altered after wounding (>2-fold change, posterior probability of differential expression [PPDE] > 0.95; Supplemental Table S1). A total of 745 probe sets were up-regulated and 382 were down-regulated. In agreement with our observations in Figure 5, A and B, *AtWRKY40* (131-fold), *AtOM66* (9.7-fold), and *AtWRKY15* (2.1-fold) were significantly induced within 10 min after wounding, with *AtWRKY40* being the second most induced gene across the genome. In contrast, *AOX1a* and *UGT74E2* were not induced significantly, which confirms the specificity of the response and similarity with our experiments. A study looking at changes in gene expression within 5 min of wounding also noted a significant induction of *AtWRKY40* using both Agilent microarrays and qRT-PCR (Walley et al., 2007).

In another study, 4-week-old plants were touched by gently folding back and forth the leaves, not damaging them (Lee et al., 2005). Samples were collected 30 min after treatment. The authors reported that expression of 589 genes was significantly touch-induced, while 171 were repressed. *AtWRKY40* (43-fold), *AtOM66* (10.7-fold), and *AtWRKY15* (4.3-fold) were also found to be significantly touch-induced, while *AOX1a* and *UGT74E2* were not. In conclusion, the rapid first peak observed in Figure 5 appears to reflect touch and wounding responses, which affects approximately 3 to 5% of the Arabidopsis transcriptome. This includes induction of several genes encoding mitochondrially targeted proteins, including *AtOM66*, as well as mitochondrial dicarboxylate substrate carriers (*DIC2*, 48-fold; *DIC1*, 21-fold; PPDE > 0.99), which are thought to provide the primary sources of reductant for mitochondrial function (Palmieri et al., 2008).

Touch Responses Directly Affect Substrate Levels and the Expression of Genes for Transporters for Energy Metabolism

Our initial interest in the early touch response was the strong induction of *AtOM66*, which encodes a mitochondrial protein. Touch responses caused by physical manipulation with water jets result in almost immediate mitochondrial and cytosolic Ca^{2+} spikes (Logan and Knight, 2003; Loro et al., 2012). This suggests mechanical manipulations may directly affect mitochondrial function. The touch- and wounding-related microarray expression data suggest that mitochondrial dicarboxylate carriers (*DICs*) are among the most highly induced genes (Lee et al., 2005). Therefore, we tested if transcripts for the three Arabidopsis *DIC* genes are responding to the mock spray treatment presented in Figure 5B. *DIC2* was induced 91-fold, *DIC1* was induced 17-fold, and *DIC3* was induced 25-fold (Fig. 6). We also tested a chloroplast-located Glc-6-phosphate transporter, *GPT2*, reported to be crucial for metabolic readjustment during dynamic acclimation (Athanasiou et al., 2010). *GPT2* was 13-fold induced by touch treatment. Together, these findings suggest that transcriptional changes during touch responses are directed to modulate import/export of metabolic substrates from energy organelles.

To confirm if touch responses indeed affect mitochondrial metabolism, metabolite levels were analyzed in the same samples used for the detailed mock spray time course used in Figure 5B (Fig. 6). In line with the strong touch-induced expression of *DIC* transcripts, several of their major substrates, including succinate and citrate, decreased in abundance approximately 2-fold within 10 min ($P < 0.05$). These metabolite levels started recovering after 30 min and returned to normal

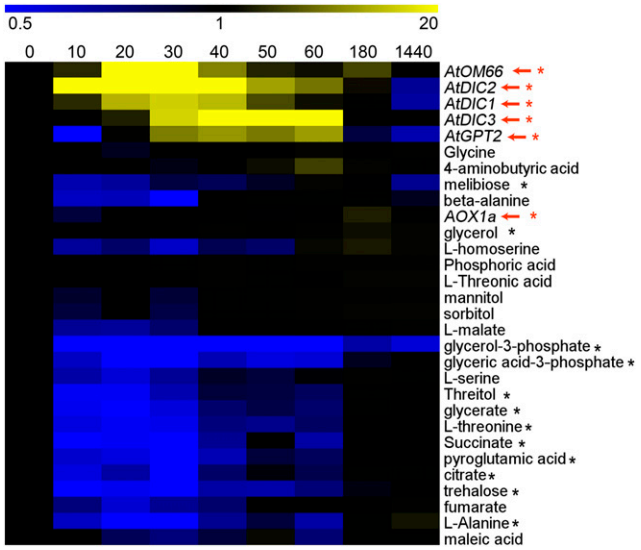

Figure 6. Touch responses are coupled to rapid changes in energy metabolism. Heat map of metabolite and transcript levels at indicated intervals (in minutes) after mock spray treatment, after hierarchical clustering (Pearson correlation and average linkage). Values represent fold changes normalized to 0 min time point. Asterisks indicate differential abundance during at least one of the time points ($P < 0.05$). Transcript levels are indicated by red arrows to differentiate from metabolites ($n = 3$).

levels by 3 to 24 h. A number of amino acids, such as L-Ala and L-Thr, followed a similar trend, while other components such as glycerol showed increases toward the later time points. These results indicate that touch responses can affect mitochondria both through substrate availability and transcriptional signaling as part of a wider cellular response.

AtWRKY15 and AtWRKY40 Are Involved in Regulation of Touch Responses

To assess if the previously identified regulators could affect touch-related expression, *AtOM66* expression was measured in the time course experiment with antimycin A treatment (Figs. 2 and 7; $n = 3$). At the 3 h time point, *anac017* plants again showed a complete loss of *AtOM66* induction, whereas none of the tested WRKY lines negatively affected *AtOM66* induction. Similar reduced *AtOM66* levels were observed during a treatment time course using two independent alleles of *anac017* mutants grown in soil (Supplemental Fig. S2C). However, loss of ANAC017 function had no effect on the touch-related peak at 30 min. This indicated that two separated signaling cascades were involved in these transcriptional responses. None of the transgenic lines tested above had a completely repressed touch-response peak, but our screen suggested that plants overexpressing *AtWRKY15* and *AtWRKY40* had an attenuated response (Fig. 7A). Due to the highly transient nature of the touch response resulting in rapid changes in *AtOM66* expression within minutes (see Fig. 5), the interexperiment variability caused these differences between *AtWRKY15 OE* or *AtWRKY40 OE* and Col-0 at the 30 min time point not to pass a standard unpaired *t* test. However, within each of three experiments the *AtOM66* expression values in *AtWRKY15 OE* and *AtWRKY40 OE* were consistently lower than in Col-0 and were found to show significantly reduced induction compared to Col-0 by a paired *t* test ($P < 0.05$).

To identify other regulators of the rapid touch responses, we carried out transcriptomic analysis focusing on the first 60 min following spray treatment. A range of mutants with previously described roles potentially relating to very early touch and wounding responses were included (see "Discussion" for more details): touch-related plasma membrane Ca^{2+} channels *mca1 mca2*, extracellular ATP receptor *atdorn1-3*, *OXDORN1* (*AtDORN1* overexpressor), and *coi1* (coronatine-insensitive jasmonic acid [JA] receptor). Two-week-old in vitro-grown seedlings were mock spray treated and triplicate pools of plants were collected at 0, 30, and 60 min. mRNA abundance of touch-response marker genes was measured by qRT-PCR analysis (Fig. 7B; Supplemental Fig. S4). Overexpression lines of *AtWRKY15* and *AtWRKY40* (independent allele) were also included and again displayed a significant reduction of *AtOM66* expression at 30 min after treatment (~35% reduction; $P < 0.05$). In contrast to our expectations, a significantly higher induction was found in *atdorn1-3* plants (~50% increase; $P = 0.01$), while the *OXDORN1* line did not show any significant differences (Fig. 7B). Homozygosity of the T-DNA insertion in *atdorn1-3* was confirmed by PCR, and *AtDORN1* transcript levels were confirmed to be overexpressed in *OXDORN1* plants (Supplemental Fig. S4). *AtWRKY40* induction at 30 min was 50% reduced in *AtWRKY15 OE* plants ($P < 0.01$) and 42% more induced in *atdorn1-3* plants (Fig. 7B). Also, *AtWRKY15* induction was significantly repressed in *AtWRKY40 OE* plants (~55% reduction; $P < 0.05$). The *mca1 mca2* and *coi1* plants showed no significant differences compared to the wild type (Fig. 7B). A mutant in gibberellin oxidase *ga2ox7* that was recently reported to be involved in touch signaling (Joao Pimenta Lange and Lange, 2015) was also analyzed, but no significant effect in transcriptional touch responses were observed compared to Col-0 at 25 min (Supplemental Fig. S4). In conclusion, our results show that AtWRKY40 and AtWRKY15 are negative regulators of touch-induced transcriptional responses.

DISCUSSION

Of several previously identified transcription factors involved in mitochondrial retrograde signaling in response to organelle inhibition, ANAC017 appears to be the main positive transcriptional regulator known to date. ANAC017 is most strongly expressed and appears to be epistatic over ANAC013 and ANAC053, as loss of ANAC017 abolishes their stress induction. This is in

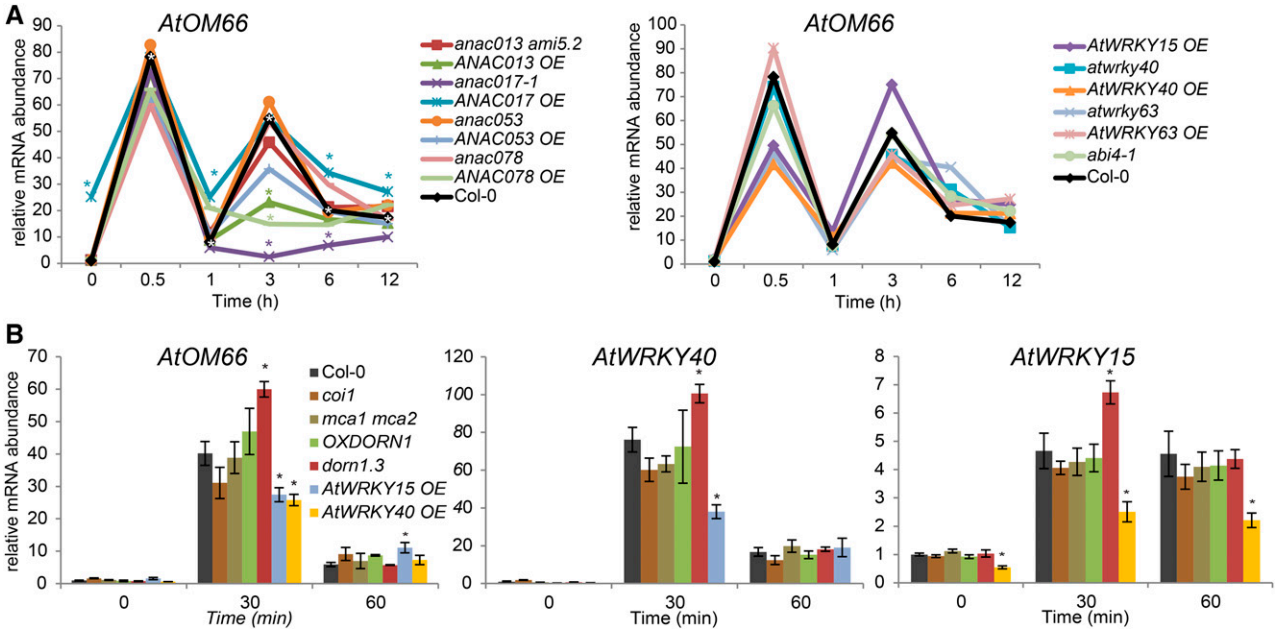

Figure 7. AtWRKY15 and AtWRKY40 modulate touch-responsive gene expression. A, Two-week-old in vitro-grown seedlings were spray treated with antimycin A. Pooled plants were collected, and mRNA levels were measured by qRT-PCR ($n = 3$) and normalized to Col-0 untreated samples (0 h). B, Two-week-old seedlings of different genotypes were spray-treated and pools of plants were collected in triplicate before treatment and at the indicated times after treatment. mRNA levels were calculated by qRT-PCR (±SE) and normalized to Col-0 untreated samples (0 h). Statistical significance is indicated by asterisks: $*P < 0.05$, $**P \leq 0.01$, and $***P < 0.001$.

line with the direct binding of the *ANAC013* promoter by ANAC017 as reported previously (De Clercq et al., 2013), and the *ANAC053* promoter contains a consensus ANAC017 mitochondrial dysfunction DNA motif binding site. At 3 h after treatment, the downstream target genes show an almost complete lack of induction in *anac017* lines compared to wild-type plants. Some weak induction at 6 h is observed, which may be due to the partial redundancy with the other NAC family members, mainly ANAC013, ANAC053, and/or ANAC078. The later increase in signal may occur through a positive feedback loop by ANAC013 as it binds and stimulates its own promoter (De Clercq et al., 2013), which may take some hours to reach a noticeable threshold in the absence of ANAC017. As previously published, ABI4 appeared to have a significant repressive effect mainly on *AOX1a* in untreated conditions (Giraud et al., 2009). The role of WRKY transcription factors in response to mitochondrial inhibition is less clearly defined during the 3 to 6 h gene expression peak. This may be due at least in part to the large redundancy within the WRKY gene family, as previous studies have shown that more than 10 different WRKY proteins can bind the promoters of *AOX1a* and *AtOM66* (Van Aken et al., 2013). For instance, AtWRKY40 is known to form a functional complex with related proteins AtWRKY18 and AtWRKY60 (Xu et al., 2006). Analysis of root growth also showed that ANAC017, and to a lesser extent ANAC013, provided the plants with enhanced resistance to inhibitors of organelle function. Altered expression of a number of transcription factors resulted in reduced root growth (Fig. 3), which likely reflected a perturbation of basal gene expression resulting in mild growth penalties to the plants.

Our previous analysis suggested that the role of ANAC017 in stress signaling is mostly confined to regulation of gene expression after mitochondrial function was inhibited at the level of Complex III (antimycin A), Complex IV (myxothiazol), and/or the TCA cycle (MFA; Ng et al., 2013b). The experiments shown here suggest that the role of ANAC017 may stretch further than just mitochondrial dysfunction, as shown by the very clear inhibition of stress signaling in response to chloroplast superoxide generator MV (Tsang et al., 1991). MV induces a transfer of electrons from photosystem I to oxygen in illuminated conditions, resulting in superoxide generation and oxidative stress that harms chloroplast function. The lack of mitochondrial stress marker gene induction (e.g. *AOX1a* and *AtOM66*) following treatment with MV compared to the mock treatment further supports that MV triggered signaling in the light is largely independent of mitochondria. Nevertheless, ANAC017 does not seem to mediate the signals for every type of stress that induces ANAC017 target genes. Stress response triggers such as UV, salicylic acid, cold, abscisic acid, and Flg22 can also induce gene expression, e.g. *AOX1a* expression (Ng et al., 2013b; this study). However, loss of ANAC017 did not significantly reduce the induction of *AOX1a* to many of these triggers (Ng et al., 2013b). From our

results ANAC017 is also not involved in every type of chloroplast retrograde response. High light stress causes a rapid induction within 1 h of many of the same target genes as MV (e.g. *HSP17.6A*, *HSP17.6 CII*, *TINY TF*, and dual-targeted *sHSP23.5*); however, loss of ANAC017 function did not significantly reduce these high light responses, nor did *anac017* plants have a GUN phenotype in our assays. Evidently, these genes are steered by separate pathways in the case of MV or high light, but have similar gene expression outcomes, providing an elegant example of convergent signaling. Previous reports also suggested a large overlap between target genes of ANAC017 and singlet oxygen-induced genes in the *flu* mutant (Meskauskiene et al., 2001; Ng et al., 2013b). Our results indicate that both ANAC017 and *flu*-mediated signaling may converge on multiple common target genes, but the signaling cascades that lead there appear to be distinct, shedding further light on the apparent cross talk between different ROS stress signaling pathways (Laloi et al., 2007; Lee et al., 2007). Indeed, several of these genes contain consensus ANAC017 binding sites [CA(A/C)G] in their promoters, such as *HSP17.6A* and *sHSP23.5*.

Our results also raise the question of whether the ANAC017 pathway requires energy organelle dysfunction as part of the signaling event. Perhaps ANAC017 on the ER membrane receives inputs from many different upstream signaling pathways, of which organellar dysfunction, ER stress, or unfolded protein responses may be some examples (Senft and Ronai, 2015). To a large extent, the cell can distinguish the source of the stress despite the fact that ANAC017 is mediating multiple signals and overlapping target genes. This is evident from the observation that treatment with antimycin A or MV causes very different levels of induction of ANAC017 target genes: e.g. *AOX1a* and *AtOM66* are 4- to 10-fold more induced by antimycin A than by MV, while *HSP17.6A* and *HSP17.6 CII* are 8- to 16-fold more induced by MV than antimycin A (Supplemental Fig. S5; Fig. 4). It appears that additional (currently unknown) factors may codetermine the specificity of ANAC017.

Unexpectedly, gene expression of mitochondrial and chloroplast proteins also responded to a much more immediate transient signaling cascade. This transient expression was initiated within 10 min of inhibitor application and appeared uncoupled from the organellar inhibition caused later on by the active compound. Again, overlapping genes with organelle inhibitor-induced expression were affected (e.g. *AtOM66*), but distinct pathways lead to activation, implying convergent signaling. This rapid response is very similar to mechanical manipulation signaling, such as touch and wounding responses, which induce Ca^{2+} spikes in mitochondria within seconds (Logan and Knight, 2003). Our control experiments showed that while water treatment induced the largest signaling responses, other mechanical processes also yielded significant responses (Fig. 5). Overall the effects observed here appeared to be proportional to the degree of mechanical stimulation. Touch-responsive gene expression was first described in the literature several decades ago (Braam and Davis, 1990), but only limited information on the genes that directly regulate these very rapid gene expression responses has been published. A number of studies suggested that plasma membrane-located Ca^{2+} transporters MCA1 and MCA2 are involved in touch responses and loss-of-function *mca1 mca2* mutants showed impaired mechanosensing (Nakagawa et al., 2007). An extracellular ATP (eATP) receptor AtDORN1, also on the plasma membrane, rapidly relays the presence of eATP (which is known to be released upon wounding) and triggers transcriptional responses (Choi et al., 2014), including induction of *AtWRKY15*, *AtWRKY40*, and *AtOM66*. Phytohormones are also thought to be involved in touch responsiveness, and plants show altered morphology and pest resistance when touched on a regular basis, a process termed thigmomorphogenesis (Chehab et al., 2012). JA and gibberellic acid (GA) are thought to be main contributors to thigmomorphogenesis, but it is unclear whether JA or GA signaling is also involved in the very early transcriptional responses (Chehab et al., 2012; Joao Pimenta Lange and Lange, 2015).

Here, we found that AtWRKY40 and AtWRKY15 may play repressive roles in the early touch response. Their transcripts are strongly induced by the touch treatment itself, suggesting that they may contribute to the rapid decline of mRNA expression between 30 and 60 min after treatment. We selected 10 of the most strongly induced touch-responsive genes, as identified by Lee et al. (2005) (Supplemental Fig. S6), for a more detailed promoter analysis, including *AtOM66*, *DIC1*, *DIC2*, *AtWRKY40*, and *AtWRKY15.* In line with a direct role for WRKY transcription factors in touch responses, all 10 genes contained W-boxes (TTGACY) in their 1-kb upstream promoter region ($P < 0.004$) using the Athena tool (O'Connor et al., 2005). Accordingly, the promoter of *AtOM66* was previously demonstrated to be directly bound by AtWRKY15 and AtWRKY40 (Van Aken et al., 2013). The presence of WRKY binding sites in stress-responsive genes encoding energy organelle proteins has been described previously (Van Aken et al., 2009; Leister et al., 2011; Van Aken and Whelan, 2012). However, not all these genes exhibit touch-responsive expression patterns (e.g. *AOX1a*), suggesting that WRKY transcription factors play complex roles in multiple signaling cascades.

Although several of the genes induced by touch responses play important roles in biotic and abiotic stress responses, the touch response also targets energy organelle function and substrates for metabolism (Xu et al., 2006; Shang et al., 2010; Sheard et al., 2010; Zhang et al., 2014). All three DICs in Arabidopsis are highly induced by touch responses. DICs are the main transporters that allow substrates such as succinate, malate, oxaloacetate, and 2-oxoglutarate to pass the inner mitochondrial membrane, in exchange for anions including phosphate, sulfate, and arsenate (Palmieri et al., 2008). DICs can also function in exporting TCA intermediates as substrates for anaplerotic metabolism. For

instance, DICs transport 2-oxoglutarate, which is important for anaplerotic pathways and nitrogen cycling, as well as malate for photorespiration and reductant exchange with chloroplasts. A metabolite analysis revealed that DIC substrates such as succinate and citrate are significantly reduced within 10 min of spray treatment, indicating that such rapid transcriptional responses occur to address a physiological change. Citrate is also known to trigger specific transcriptional response, but the target genes appear not to overlap with our findings, and the timeframe of 8 h used in these experiments is different (Finkemeier et al., 2013).

Rapid (<1 h) transient changes in organic acid contents in Arabidopsis seedlings in response to CO_2 levels have also been reported, further showing that such dynamic responses in the metabolome are possible (Dutta et al., 2009). Recent metabolic studies have suggested a role for dicarboxylates in rapid respiratory responses to Pi starvation, and DICs are indeed induced within 1 h of transfer of plants to Pi depleted medium (Lin et al., 2011; Alexova et al., 2015). Rapid transcriptional responses within 10 min have also been found in response to high-light treatment and involve chloroplast-located triose phosphate/phosphate translocator (TPT; Vogel et al., 2014). Another gene related to energy metabolism and transport that is highly touch-responsive is the plastid Glc-6-phosphate translocator *GPT2*. GPT2 is involved in regulating transitions in metabolic states, with plants lacking GPT2 being unable to undergo dynamic photosynthetic acclimation under naturally viable conditions (Athanasiou et al., 2010). This further underlines the importance of short-term responses in maintaining plant energy organelle function.

Taken together, these findings suggest that rapid touch and wounding responses could prepare energy metabolism for a change in substrate availability and potentially redirect nutrients and substrates from primary catabolic processes to secondary metabolism or biosynthesis. Touch-induced transcriptional responses are closely related to dark-shift responses (Lee et al., 2004), which also target *AtWRKY40*, *DIC2*, and *AtOM66*. Such a shift in light input could have dramatic effects on energy metabolism that need to be addressed quickly, perhaps by shifting to anaplerotic mitochondrial metabolism and usage of starch reserves, to allow sustained energy supply for the cell (Athanasiou et al., 2010). Plants thus seem to use overlapping signaling systems to respond to metabolic changes and biotic stress. Recent work showed that plants respond rapidly to even just the leaf vibrations caused by insect herbivores (Appel and Cocroft, 2014). Such a mechanical signal can travel much faster through the plant than, for example, phytohormones. From this perspective, touch, wounding, and dark-shift responses may all precede similar challenges, thus initiating overlapping defense responses that would have advantages for the plant.

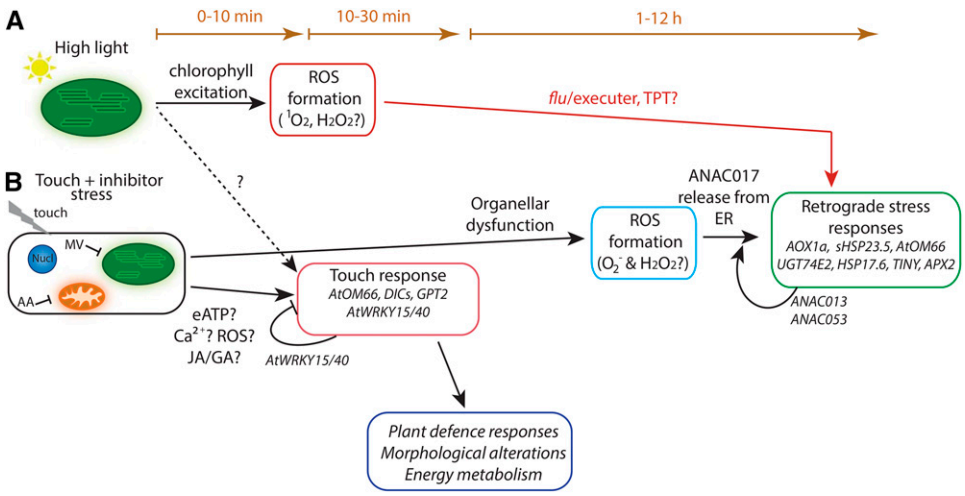

Figure 8. A working model for retrograde, high light-, and touch-responsive operational control in plants. A, High light treatment leads to chlorophyll overexcitation and reactive oxygen species (ROS) production. Signals are transduced to the nucleus possibly via *flu*/executer or TPT signaling, leading to retrograde transcriptional responses. B, Mechanical stress (e.g. by touch or spray application of an exogenous compound) triggers a transcriptional response within minutes. Studies suggest signaling molecules such as Ca^{2+}, eATP, ROS, JA, and GA are involved. This first touch response is likely to be of key importance for stress recognition, successful pathogen resistance, morphological alterations, and rapid readjustments of energy metabolism. A second, independent signaling network caused by the active inhibitor compound (e.g. affecting mitochondria and/or chloroplasts such as antimycin A [AA] and MV) then launches a more general stress response, possibly dependent on ROS, via activation of NAC transcription factors present on the ER. NAC target genes are at least partially overlapping with high light-induced genes, but different signaling pathways are involved.

CONCLUSION

In conclusion, we found that multiple independent signaling pathways operate following a wide range of treatments that involve physical manipulations, changes in light intensity, and inhibitor/elicitor treatments (Fig. 8). The first gene expression peak within 10 min after physical manipulation or dark shifts is clearly related to pathogen defense signaling and appears to be regulated at least in part by WRKY transcription factors. Our study shows that this first expression phase may also facilitate rapid readjustments in energy metabolism and energy organelle functions, as plants anticipate or respond to changes in substrate or nutrient availability very soon after a manipulation. A second signaling system occurs around 3 to 6 h after chemical chloroplast or mitochondrial inhibition and is regulated to a large extent by ANAC017. This peak affects, e.g. *AOX1a*, heat shock proteins, chaperones etc., and appears enriched in gene products primarily associated with repairing/maintaining the energy organelle machinery. This response may thereby prevent excessive ROS production during functional inhibition, rather than optimizing substrate availability and usage. A third response triggered by excessive light, which causes damage to the photosystems, induces overlapping genes with the second pathway. However, this high light pathway is ANAC017-independent and may at least partly be coordinated by the *flu*/executer and/or TPT pathways (Meskauskiene et al., 2001; Lee et al., 2007; Vogel et al., 2014). Our results extend the idea that retrograde signals affect organelle biogenesis (biogenic control) or organelle performance (operational control; Pogson et al., 2008), postulating that operational control involves separate signaling pathways for opportunity and risk (metabolic substrate availability and pathogen defense regulated, e.g. by WRKYs) and for damage repair (organelle inhibitors, high light, and ETC disruption regulated, e.g. by NACs).

MATERIALS AND METHODS

Materials and Growth Conditions

Arabidopsis (*Arabidopsis thaliana*) Col-0 was used in all experiments. Seeds were sown on soil mix or MS media with 2% Suc and stratified for 2 to 3 d at 4°C, then grown under long-day conditions (16 h light/8 h dark) at 22°C and 100 μmol m^{-2} s^{-1}. Previously published transgenic lines were obtained from Ng et al. (2013b) (*anac017*: *rao2.1*; *anac017-2*: SALK_022174), De Clercq et al. (2013) (*anac013 amiRNA5.2*, *ANAC013 OE6*, *ANAC053 OE*, and *ANAC078 OE*), Van Aken et al. (2013) (*AtWRKY15 OE1*, *atwrky40*, *AtWRKY40 OE2*, *atwrky63*, and *AtWRKY63 OE1*), Giraud et al. (2009) (*abi4-1*), Choi et al. (2014) (*atdorn1.3* and *OXDORN1*), and Yamanaka et al. (2010) (*mca1 mca2*). *coi1-1* was kindly provided by Dr. Louise Thatcher (CSIRO, Western Australia). We are grateful to Dr. Gary Stacey (University of Missouri), Dr. Roberto Solano (Centro Nacional de Biotecnología, Spain), Dr. Kemal Kazan (CSIRO Agriculture Flagship, Australia), and Dr. Hidetoshi Iida (Tokyo Gakugei University, Japan) for promptly sharing transgenic materials. *Anac053* (SALK_009578), *anac078* (SALK_025098), and *ga2ox7* (SALK_055721C) were obtained from NASC. *ANAC017 OE* plants were generated by cloning the full-length *ANAC017* coding sequence into pB7WG2 (Karimi et al., 2002) using standard Gateway (Life Technologies) cloning strategies. *ANAC017*, *ANAC078*, and *ANAC053* expression levels were tested by qRT-PCR (Supplemental Fig. S2). The 1.5-kb promoter regions of *ANAC013*, *ANAC017*, *ANAC053*, and *ANAC078* were amplified and cloned into pBGWFS7 (Karimi et al., 2002) via Gateway recombination and transformed by floral dipping as described previously (Clough and Bent, 1998; Zhang et al., 2012). At least two independent lines per construct were analyzed with comparable results. All primers used in this study are listed in Supplemental Table S2.

Stress Treatments of Plants

Seeds were sown on petri dishes containing MS media + 2% Suc, stratified for 2 to 3 d in the cold room, and then incubated in long-day growth conditions for 2 weeks. Pools of plants were then collected before or after treatment and immediately placed in liquid nitrogen for storage and further processing. For transcript analysis, plants were sprayed with mock (water + Tween), 50 μM antimycin A, 50 μM monofluoroacetate, 1 μM Flg22, 50 μM MV, or 20 μM norflurazon. For UV treatment, plants received 5 kJ/cm^2 UV radiation (254 nm) using a CX-2000 UV cross-linker (UVP Ltd.). In vitro stress assays were performed as previously described using 50 μM antimycin A, 100 μM rotenone, or 20 μM MV (De Clercq et al., 2013). Statistical analysis was performed using Student's *t* test. Additional control experiments for touch-related treatments were as follows: (1) unopened/untreated negative control, (2) plates opened for the same duration as spray treatment but otherwise untreated, (3) plates opened and gently mechanically stimulated by touching with blunt tweezers, and (4) spray treatment with water. A similar control experiment was also performed on soil-grown plants that were (1) untreated, (2) gently mechanically stimulated with blunt tweezers, and (3) spray treated with water. For high light treatment, in vitro-grown 2-week-old plants were exposed to 750 μmol m^{-2} s^{-1} for 1 h and compared to untreated control. Furthermore, to allow differentiation between high light treatment and associated increase in temperature, a heat control set was used that was exposed to normal light (100 μmol m^{-2} s^{-1}) but incubated at 28°C (the temperature that was measured in the plates during the high light treatment). For root growth assays, the different plant lines were incubated on vertically positioned plates supplemented with 50 μM antimycin A, 10 μM rotenone, and 50 μM MV. Plants stratified in the cold room for 3 d and were kept in long-day conditions for 7 d. Primary root length was measured using ImageJ. Statistical analysis was performed using Student's *t* test.

Promoter-GUS Analysis

The 1.5-kb promoter regions were cloned using standard Gateway (Life Technologies) procedures into pBGWFS7 (Karimi et al., 2002). Three-week-old in vitro-grown plants were stained for GUS activity before and 6 h after spray treatment with 50 μM antimycin A as described previously (Van Aken et al., 2007).

Quantitative RT-PCR and Microarray Analysis

RNA isolation, cDNA generation, and qRT-PCR were performed as described (Van Aken et al., 2013) using Spectrum RNA Plant extraction kits (Sigma-Aldrich), iScript cDNA synthesis kit (Bio-Rad), and a Roche LC480 light cycler using SYBRgreen detection assays. All primers for qRT-PCR are shown in Supplemental Table S2. Relative expression values were normalized with untreated Col-0 samples set as 1. Statistical analyses were performed using Student's *t* test throughout the manuscript, except where indicated. The E-GEOD-48676 microarray data set was obtained from ArrayExpress and analyzed using Cyber-T as previously described (Zhang et al., 2014). Changes were considered significant at false discovery rate correction level of PPDE ($<$P) > 0.95 and 2-fold change.

Metabolite Analysis

Approximately 20 to 30 mg of frozen tissue from pooled 2-week-old plants grown in vitro were analyzed in biological triplicate per time point after mock spray treatment using gas chromatography-mass spectrometry. Full description of metabolite analysis is available in Supplemental Methods. Data were imported and statistically analyzed in Metabolome Express (Carroll et al., 2010).

Supplemental Data

The following supplemental materials are available.

Supplemental Figure 1. UV-induced expression of retrograde-related genes.

Supplemental Figure 2. Confirmation of ANAC expression levels in transgenic lines, leaf respiration, and antimycin A response.

Supplemental Figure 3. ANAC017 is not a regulator of high light- and norflurazon-responsive gene expression.

Supplemental Figure 4. Touch-responsive gene expression.

Supplemental Figure 5. Expression patterns of dicarboxylate carriers and HSP17.6 during antimycin A treatment.

Supplemental Figure 6. Promoter analysis of touch-responsive genes.

Supplemental Table 1. Wounding microarray analysis.

Supplemental Table 2. RT-PCR primers.

Supplemental Methods.

ACKNOWLEDGMENTS

We thank Dorothee Hahne of Metabolomics Australia for performing the gas chromatography-mass spectrometry metabolite analysis and acknowledge the use of Metabolomics Australia facilities funded by National Collaborative Research Infrastructure Strategy and the Government of Western Australia. We thank Dr. Sandy Vanderauwera for help with transgenic NAC lines.

Received April 14, 2016; accepted May 4, 2016; published May 9, 2016.

LITERATURE CITED

Alexova R, Nelson CJ, Jacoby RP, Millar AH (2015) Exposure of barley plants to low Pi leads to rapid changes in root respiration that correlate with specific alterations in amino acid substrates. New Phytol **206:** 696–708

Appel HM, Cocroft RB (2014) Plants respond to leaf vibrations caused by insect herbivore chewing. Oecologia **175:** 1257–1266

Araújo WL, Nunes-Nesi A, Fernie AR (2014) On the role of plant mitochondrial metabolism and its impact on photosynthesis in both optimal and sub-optimal growth conditions. Photosynth Res **119:** 141–156

Athanasiou K, Dyson BC, Webster RE, Johnson GN (2010) Dynamic acclimation of photosynthesis increases plant fitness in changing environments. Plant Physiol **152:** 366–373

Blanco NE, Guinea-Díaz M, Whelan J, Strand Å (2014) Interaction between plastid and mitochondrial retrograde signalling pathways during changes to plastid redox status. Philos Trans R Soc Lond B Biol Sci **369:** 20130231

Braam J, Davis RW (1990) Rain-, wind-, and touch-induced expression of calmodulin and calmodulin-related genes in Arabidopsis. Cell **60:** 357–364

Carroll AJ, Badger MR, Harvey Millar A (2010) The MetabolomeExpress Project: enabling web-based processing, analysis and transparent dissemination of GC/MS metabolomics datasets. BMC Bioinformatics **11:** 376

Chehab EW, Yao C, Henderson Z, Kim S, Braam J (2012) Arabidopsis touch-induced morphogenesis is jasmonate mediated and protects against pests. Curr Biol **22:** 701–706

Choi J, Tanaka K, Cao Y, Qi Y, Qiu J, Liang Y, Lee SY, Stacey G (2014) Identification of a plant receptor for extracellular ATP. Science **343:** 290–294

Clough SJ, Bent AF (1998) Floral dip: a simplified method for Agrobacterium-mediated transformation of *Arabidopsis thaliana*. Plant J **16:** 735–743

Comelli RN, Welchen E, Kim HJ, Hong JC, Gonzalez DH (2012) Delta subclass HD-Zip proteins and a B-3 AP2/ERF transcription factor interact with promoter elements required for expression of the Arabidopsis cytochrome c oxidase 5b-1 gene. Plant Mol Biol **80:** 157–167

Dahal K, Wang J, Martyn GD, Rahimy F, Vanlerberghe GC (2014) Mitochondrial alternative oxidase maintains respiration and preserves photosynthetic capacity during moderate drought in Nicotiana tabacum. Plant Physiol **166:** 1560–1574

De Clercq I, Vermeirssen V, Van Aken O, Vandepoele K, Murcha MW, Law SR, Inzé A, Ng S, Ivanova A, Rombaut D, et al (2013) The membrane-bound NAC transcription factor ANAC013 functions in mitochondrial retrograde regulation of the oxidative stress response in Arabidopsis. Plant Cell **25:** 3472–3490

Dojcinovic D, Krosting J, Harris AJ, Wagner DJ, Rhoads DM (2005) Identification of a region of the Arabidopsis AtAOX1a promoter necessary for mitochondrial retrograde regulation of expression. Plant Mol Biol **58:** 159–175

Dutta B, Kanani H, Quackenbush J, Klapa MI (2009) Time-series integrated "omic" analyses to elucidate short-term stress-induced responses in plant liquid cultures. Biotechnol Bioeng **102:** 264–279

Finkemeier I, König AC, Heard W, Nunes-Nesi A, Pham PA, Leister D, Fernie AR, Sweetlove LJ (2013) Transcriptomic analysis of the role of carboxylic acids in metabolite signaling in Arabidopsis leaves. Plant Physiol **162:** 239–253

Giraud E, Ng S, Carrie C, Duncan O, Low J, Lee CP, Van Aken O, Millar AH, Murcha M, Whelan J (2010) TCP transcription factors link the regulation of genes encoding mitochondrial proteins with the circadian clock in *Arabidopsis thaliana*. Plant Cell **22:** 3921–3934

Giraud E, Van Aken O, Ho LH, Whelan J (2009) The transcription factor ABI4 is a regulator of mitochondrial retrograde expression of ALTERNATIVE OXIDASE1a. Plant Physiol **150:** 1286–1296

Ho LH, Giraud E, Uggalla V, Lister R, Clifton R, Glen A, Thirkettle-Watts D, Van Aken O, Whelan J (2008) Identification of regulatory pathways controlling gene expression of stress-responsive mitochondrial proteins in Arabidopsis. Plant Physiol **147:** 1858–1873

Howell KA, Narsai R, Carroll A, Ivanova A, Lohse M, Usadel B, Millar AH, Whelan J (2009) Mapping metabolic and transcript temporal switches during germination in rice highlights specific transcription factors and the role of RNA instability in the germination process. Plant Physiol **149:** 961–980

Ishizaki K, Schauer N, Larson TR, Graham IA, Fernie AR, Leaver CJ (2006) The mitochondrial electron transfer flavoprotein complex is essential for survival of Arabidopsis in extended darkness. Plant J **47:** 751–760

Ivanova A, Law SR, Narsai R, Duncan O, Lee JH, Zhang B, Van Aken O, Radomiljac JD, van der Merwe M, Yi K, Whelan J (2014) A functional antagonistic relationship between auxin and mitochondrial retrograde signaling regulates alternative oxidase1a expression in Arabidopsis. Plant Physiol **165:** 1233–1254

Joao Pimenta Lange M, Lange T (2015) Touch-induced changes in Arabidopsis morphology dependent on gibberellin breakdown. Nature Plants **1:** 14025

Karimi M, Inzé D, Depicker A (2002) GATEWAY vectors for Agrobacterium-mediated plant transformation. Trends Plant Sci **7:** 193–195

Kerchev PI, De Clercq I, Denecker J, Mühlenbock P, Kumpf R, Nguyen L, Audenaert D, Dejonghe W, Van Breusegem F (2014) Mitochondrial perturbation negatively affects auxin signaling. Mol Plant **7:** 1138–1150

Kilian J, Whitehead D, Horak J, Wanke D, Weinl S, Batistic O, D'Angelo C, Bornberg-Bauer E, Kudla J, Harter K (2007) The AtGenExpress global stress expression data set: protocols, evaluation and model data analysis of UV-B light, drought and cold stress responses. Plant J **50:** 347–363

Koussevitzky S, Nott A, Mockler TC, Hong F, Sachetto-Martins G, Surpin M, Lim J, Mittler R, Chory J (2007) Signals from chloroplasts converge to regulate nuclear gene expression. Science **316:** 715–719

Laloi C, Stachowiak M, Pers-Kamczyc E, Warzych E, Murgia I, Apel K (2007) Cross-talk between singlet oxygen- and hydrogen peroxide-dependent signaling of stress responses in Arabidopsis thaliana. Proc Natl Acad Sci USA **104:** 672–677

Law SR, Narsai R, Taylor NL, Delannoy E, Carrie C, Giraud E, Millar AH, Small I, Whelan J (2012) Nucleotide and RNA metabolism prime translational initiation in the earliest events of mitochondrial biogenesis during Arabidopsis germination. Plant Physiol **158:** 1610–1627

Lee D, Polisensky DH, Braam J (2005) Genome-wide identification of touch- and darkness-regulated Arabidopsis genes: a focus on calmodulin-like and XTH genes. New Phytol **165:** 429–444

Lee KP, Kim C, Landgraf F, Apel K (2007) EXECUTER1- and EXECUTER2-dependent transfer of stress-related signals from the plastid to the nucleus of *Arabidopsis thaliana*. Proc Natl Acad Sci USA **104:** 10270–10275

Leister D, Wang X, Haberer G, Mayer KF, Kleine T (2011) Intracompartmental and intercompartmental transcriptional networks coordinate the expression of genes for organellar functions. Plant Physiol **157:** 386–404

Lin WD, Liao YY, Yang TJ, Pan CY, Buckhout TJ, Schmidt W (2011) Coexpression-based clustering of Arabidopsis root genes predicts functional modules in early phosphate deficiency signaling. Plant Physiol **155:** 1383–1402

Logan DC, Knight MR (2003) Mitochondrial and cytosolic calcium dynamics are differentially regulated in plants. Plant Physiol **133:** 21–24

Loro G, Drago I, Pozzan T, Schiavo FL, Zottini M, Costa A (2012) Targeting of Cameleons to various subcellular compartments reveals a strict cytoplasmic/mitochondrial Ca^{2+} handling relationship in plant cells. Plant J **71:** 1–13

Meskauskiene R, Nater M, Goslings D, Kessler F, op den Camp R, Apel K (2001) FLU: a negative regulator of chlorophyll biosynthesis in *Arabidopsis thaliana*. Proc Natl Acad Sci USA **98:** 12826–12831

Nakagawa Y, Katagiri T, Shinozaki K, Qi Z, Tatsumi H, Furuichi T, Kishigami A, Sokabe M, Kojima I, Sato S, et al (2007) Arabidopsis plasma membrane protein crucial for Ca^{2+} influx and touch sensing in roots. Proc Natl Acad Sci USA **104:** 3639–3644

Ng S, De Clercq I, Van Aken O, Law SR, Ivanova A, Willems P, Giraud E, Van Breusegem F, Whelan J (2014) Anterograde and retrograde regulation of nuclear genes encoding mitochondrial proteins during growth, development, and stress. Mol Plant **7:** 1075–1093

Ng S, Giraud E, Duncan O, Law SR, Wang Y, Xu L, Narsai R, Carrie C, Walker H, Day DA, et al (2013a) Cyclin-dependent kinase E1 (CDKE1) provides a cellular switch in plants between growth and stress responses. J Biol Chem **288:** 3449–3459

Ng S, Ivanova A, Duncan O, Law SR, Van Aken O, De Clercq I, Wang Y, Carrie C, Xu L, Kmiec B, et al (2013b) A membrane-bound NAC transcription factor, ANAC017, mediates mitochondrial retrograde signaling in Arabidopsis. Plant Cell **25:** 3450–3471

Nomura H, Komori T, Uemura S, Kanda Y, Shimotani K, Nakai K, Furuichi T, Takebayashi K, Sugimoto T, Sano S, et al (2012) Chloroplast-mediated activation of plant immune signalling in Arabidopsis. Nat Commun **3:** 926

O'Connor TR, Dyreson C, Wyrick JJ (2005) Athena: a resource for rapid visualization and systematic analysis of Arabidopsis promoter sequences. Bioinformatics **21:** 4411–4413

Palmieri L, Picault N, Arrigoni R, Besin E, Palmieri F, Hodges M (2008) Molecular identification of three *Arabidopsis thaliana* mitochondrial dicarboxylate carrier isoforms: organ distribution, bacterial expression, reconstitution into liposomes and functional characterization. Biochem J **410:** 621–629

Pogson BJ, Woo NS, Förster B, Small ID (2008) Plastid signalling to the nucleus and beyond. Trends Plant Sci **13:** 602–609

Schwarzländer M, König AC, Sweetlove LJ, Finkemeier I (2012) The impact of impaired mitochondrial function on retrograde signalling: a meta-analysis of transcriptomic responses. J Exp Bot **63:** 1735–1750

Senft D, Ronai ZA (2015) UPR, autophagy, and mitochondria crosstalk underlies the ER stress response. Trends Biochem Sci **40:** 141–148

Shang Y, Yan L, Liu ZQ, Cao Z, Mei C, Xin Q, Wu FQ, Wang XF, Du SY, Jiang T, et al (2010) The Mg-chelatase H subunit of Arabidopsis antagonizes a group of WRKY transcription repressors to relieve ABA-responsive genes of inhibition. Plant Cell **22:** 1909–1935

Sheard LB, Tan X, Mao H, Withers J, Ben-Nissan G, Hinds TR, Kobayashi Y, Hsu FF, Sharon M, Browse J, He SY, Rizo J, Howe GA, Zheng N (2010) Jasmonate perception by inositol-phosphate-potentiated COI1-JAZ co-receptor. Nature **468:** 400–405

Skirycz A, De Bodt S, Obata T, De Clercq I, Claeys H, De Rycke R, Andriankaja M, Van Aken O, Van Breusegem F, Fernie AR, Inzé D (2010) Developmental stage specificity and the role of mitochondrial metabolism in the response of Arabidopsis leaves to prolonged mild osmotic stress. Plant Physiol **152:** 226–244

Stael S, Kmiecik P, Willems P, Van Der Kelen K, Coll NS, Teige M, Van Breusegem F (2015) Plant innate immunity–sunny side up? Trends Plant Sci **20:** 3–11

Susek RE, Ausubel FM, Chory J (1993) Signal transduction mutants of Arabidopsis uncouple nuclear CAB and RBCS gene expression from chloroplast development. Cell **74:** 787–799

Tsang EW, Bowler C, Hérouart D, Van Camp W, Villarroel R, Genetello C, Van Montagu M, Inzé D (1991) Differential regulation of superoxide dismutases in plants exposed to environmental stress. Plant Cell **3:** 783–792

Tognetti VB, Van Aken O, Morreel K, Vandenbroucke K, van de Cotte B, De Clercq I, Chiwocha S, Fenske R, Prinsen E, Boerjan W, et al (2010) Perturbation of indole-3-butyric acid homeostasis by the UDP-glucosyltransferase UGT74E2 modulates Arabidopsis architecture and water stress tolerance. Plant Cell **22:** 2660–2679

Van Aken O, Pecenková T, van de Cotte B, De Rycke R, Eeckhout D, Fromm H, De Jaeger G, Witters E, Beemster GT, Inzé D, Van Breusegem F (2007) Mitochondrial type-I prohibitins of *Arabidopsis thaliana* are required for supporting proficient meristem development. Plant J **52:** 850–864

Van Aken O, Whelan J (2012) Comparison of transcriptional changes to chloroplast and mitochondrial perturbations reveals common and specific responses in Arabidopsis. Front Plant Sci **3:** 281

Van Aken O, Zhang B, Carrie C, Uggalla V, Paynter E, Giraud E, Whelan J (2009) Defining the mitochondrial stress response in *Arabidopsis thaliana*. Mol Plant **2:** 1310–1324

Van Aken O, Zhang B, Law S, Narsai R, Whelan J (2013) AtWRKY40 and AtWRKY63 modulate the expression of stress-responsive nuclear genes encoding mitochondrial and chloroplast proteins. Plant Physiol **162:** 254–271

Vanderauwera S, Vandenbroucke K, Inzé A, van de Cotte B, Mühlenbock P, De Rycke R, Naouar N, Van Gaever T, Van Montagu MC, Van Breusegem F (2012) AtWRKY15 perturbation abolishes the mitochondrial stress response that steers osmotic stress tolerance in Arabidopsis. Proc Natl Acad Sci USA **109:** 20113–20118

Vanlerberghe GC (2013) Alternative oxidase: a mitochondrial respiratory pathway to maintain metabolic and signaling homeostasis during abiotic and biotic stress in plants. Int J Mol Sci **14:** 6805–6847

Vanlerberghe GC, McIntosh L (1992) Coordinate regulation of cytochrome and alternative pathway respiration in tobacco. Plant Physiol **100:** 1846–1851

Vogel MO, Moore M, König K, Pecher P, Alsharafa K, Lee J, Dietz KJ (2014) Fast retrograde signaling in response to high light involves metabolite export, MITOGEN-ACTIVATED PROTEIN KINASE6, and AP2/ERF transcription factors in Arabidopsis. Plant Cell **26:** 1151–1165

Walley JW, Coughlan S, Hudson ME, Covington MF, Kaspi R, Banu G, Harmer SL, Dehesh K (2007) Mechanical stress induces biotic and abiotic stress responses via a novel cis-element. PLoS Genet **3:** 1800–1812

Xu X, Chen C, Fan B, Chen Z (2006) Physical and functional interactions between pathogen-induced Arabidopsis WRKY18, WRKY40, and WRKY60 transcription factors. Plant Cell **18:** 1310–1326

Yamanaka T, Nakagawa Y, Mori K, Nakano M, Imamura T, Kataoka H, Terashima A, Iida K, Kojima I, Katagiri T, Shinozaki K, Iida H (2010) MCA1 and MCA2 that mediate Ca2+ uptake have distinct and overlapping roles in Arabidopsis. Plant Physiol **152:** 1284–1296

Yoshida K, Noguchi K (2009) Differential gene expression profiles of the mitochondrial respiratory components in illuminated Arabidopsis leaves. Plant Cell Physiol **50:** 1449–1462

Zhang B, Carrie C, Ivanova A, Narsai R, Murcha MW, Duncan O, Wang Y, Law SR, Albrecht V, Pogson B, et al (2012) LETM proteins play a role in the accumulation of mitochondrially encoded proteins in *Arabidopsis thaliana* and AtLETM2 displays parent of origin effects. J Biol Chem **287:** 41757–41773

Zhang B, Van Aken O, Thatcher L, De Clercq I, Duncan O, Law SR, Murcha MW, van der Merwe M, Seifi HS, Carrie C, et al (2014) The mitochondrial outer membrane AAA ATPase AtOM66 affects cell death and pathogen resistance in *Arabidopsis thaliana*. Plant J **80:** 709–727

Supplementary Methods

Metabolite analysis

Approx. 20-30 mg of frozen tissue from pooled two-week old plants grown in vitro were analysed in biological triplicate per time point after mock spray treatment. Metabolites were extracted using 500 µL extraction solution per 30 mg of FW (90% Methanol with 3 ISTD (abbreviation?), 100 µM labelled valine, 10 µM labelled sorbitol, 10 µM ribitol); volume of the extraction solution was adjusted to the sample weight. Samples were incubated 20 min at 65ºC and 1250 rpm incubation in a thermomixer, then centrifuged for 3 min at 20.800 g. 60 µL of supernatant was transferred into a glass insert and evaporated to dryness in a vacuum evaporator for 3 h at RT. Glass inserts were transferred to a 2 mL GC vial and capped with magnetic crimp top. Samples were derivatised using a CTC autosampler: 20 µL of 20 mg/mL methoxylamine in pyridine were added. Samples were incubated at 37ºC for 2 h and 750 rpm in the agitator. Then 20 µL N-Methyl-N-(trimethylsilyl) trifluoroacetamide (MSTFA) was added and incubated at 37ºC for 30 min and 750 rpm in the agitator. After 1 h incubation at RT 1 µL was injected onto the GC/MS. The samples were run on a 7890A GC coupled to a 5975C MSD (Agilent), the column used was a VF 5ms 30 m x 250 µm x 0.25 µm with a 10 m guard column (Agilent J&W). The carrier gas was helium and the column flow was 1mL/min. The temperature gradient of the oven was 70ºC for 1 min, then 7ºC per minute to 325ºC. The inlet, thermal auxiliary, MS source and MS quadrupole temperatures were set to 250 ºC, 280 ºC, 230 ºC and 150 ºC, respectively. The scan range was m/z 50-600. Sample input concentration was corrected using chlorophyll spectrometric measurements of the methanol extractions. Data were imported and analysed in Metabolome Express (Carroll et al., 2010).

Carroll, A.J., Badger, M.R., and Harvey Millar, A. (2010). The MetabolomeExpress Project: enabling web-based processing, analysis and transparent dissemination of GC/MS metabolomics datasets. BMC Bioinformatics **11,** 376.

Accession Numbers

Sequence data from this article can be found in the EMBL/GenBank data libraries under accession numbers listed in Supplementary Methods.

Gene Name	AGI
ANAC013	AT1G32870
ANAC016	AT1g34180
ANAC017	AT1G34190
ANAC053	AT3G10500
ANAC078	AT5G04410
AtWRKY15	AT2G23320
AtWRKY40	AT1G80840
AtWRKY63	AT1G66600
ABI4	AT2G40220
AOX1a	AT3G22370
UGT74E2	AT1G05680
AtOM66	AT3G50930
COI1	AT2G39940
AtDORN1	AT5G60300
GPT2	AT1G61800
DIC1	AT2G22500
DIC2	AT4G24570
DIC3	AT5G09470
MCA1	AT4G35920
MCA2	AT2G17780
GA2OX7	AT1G50960
AtMTM1	AT4G27940
HSP17.6 A	AT5G12030
HSP17.6 CII	AT5G12020
sHSP23.5	AT5G51440
TINY	AT5G25810
AtWRKY33	AT2G38470
AtWRKY30	AT5G24110
AtAPX2	AT3G09640

Supplementary Table 1. Microarray analysis of wounding response data set E-GEOD-48676.

Supplementary Table 2. RT-PCR primers

PrimerName	Sequence
AOX1a_RTPCR_FWD	GACGGTCCGTACGGTTTCG
AOX1a_RTPCR_REV	CTTCTGATTCGCGTCCTCCTCCT
AtMTM1_RTPCR_FWD	GCAAGAACAAGAAGACAGATAGAGAAG
AtMTM1_RTPCR_REV	TCCCATGAACAGTCCTCTCA
AtAPX2_RTPCR_FWD	TGATGTGAAGACGAAGACAGGAGGAC
AtAPX2_RTPCR_FWD	CCCATCCGACCAAACACATCTCTTA
AtOM66_RTPCR_FWD	TGCTGAGACCAGGACGTATG
AtOM66_RTPCR_REV	ACCTTCCTCGATCTTGCTGA
DIC1_RTPCR_FWD	TGGAGAAAGGGTTGTTGAAAG
DIC1_RTPCR_REV	CAACAGGATTACTCGCAACG
DIC2_RTPCR_FWD	TTGAAATAGTGAACACAAGAAGGAA
DIC2_RTPCR_REV	TTGTATTTAACAACAATGCTTGAACA
DIC3_RTPCR_FWD	AACGAAGGTGGACTGATCAAC
DIC3_RTPCR_REV	AGGATTCCCGACGACTGAT
DORN_SALK042209_LP	CTGAATACTTGCGTCTCCTGC
DORN_SALK042209_RP	CAGCTTGCGAGGTTATGATTC
DORN1_RTPCR_FWD	TGCAGAAGATCCTCAGTCCA
DORN1_RTPCR_REV	GACAGATGAAAACAATATTGAGAGCTA
GPT2_RTPCR_FWD	CCGTGGAAGGTCCTCAAAT
GPT2_RTPCR_REV	TTTGTGCCACTACCCACCA
HSP17.6A_RTPCR_FWD	CTTCAAGAGCTTACATGCGAGA
HSP17.6A_RTPCR_REV	GCTCGATAACGTCAGCTGGT
HSP17.6-CII_RTPCR_FWD	ACCCTTCACGAGTTTACATGC
HSP17.6-CII_RTPCR_REV	CGATGACGTCAGCAGGTG
NAC13-RT-PCR-F	CCATAGAGGCAGGGCACCTAATGG
NAC13-RT-PCR-R	CCATTCTTAGGACCAGACCCAC
NAC16-RT-PCR-F	CTGGTTATTGGAAGGCGACAGG
NAC16-RT-PCR-R	CTCCCTAGCTCTTCTTCATCC
NAC17-RT-PCR-F	TCAGGTGTGATGCCTGATTCCAC
NAC17-RT-PCR-R	AGCCGATGAGAACTGGCTTGTTG
NAC53-RT-PCR-F	GACTACAGGGAAAGATCGAGAG
NAC53-RT-PCR-R	GGTGAACACCAGTTTTATCAAGG
NAC78-RT-PCR-F	CGATATTGATGACATTGACGAGA
NAC78-RT-PCR-R	CTTGATTCCCCATGACAATAGTT
TINY_RTPCR_FWD	CGTGACCGTCTCTGGTTAGG
TINY_RTPCR_REV	CAGAAGAAAGCAACGTCGTG
UBC_RTPCR_FWD	CTGCGACTCAGGGAATCTTCTA
UBC_RTPCR_REV	TTGTGCCATTGAATTGAACCC
WRKY15_RTPCR_FWD	ATCTTCTCACCGGAAAATGC

WRKY15_RTPCR_REV	CGCCGGAACCCTAATTATTC
WRKY30_RTPCR_FWD	TCCGATCAAGAACCACTTGTC
WRKY30_RTPCR_REV	CGTCCAGCGTTCTATCAACA
WRKY33_RTPCR_FWD	GGGAAACCCAAATCCAAGA
WRKY33_RTPCR_REV	GTTTCCCTTCGTAGGTTGTGA
WRKY40_RTPCR_FWD	CCAAGAGCTTACTTCAAATGTGC
WRKY40_RTPCR_REV	CTGATCCTCCACACTTCTCTGA
WRKY63_RTPCR2_FWD	GCAGGTCTTGTGCCTCAAAG
WRKY63_RTPCR2_REV	GGAATCATCTCTGTAAATCTCTAAAC
sHSP23.5_RTPCR_REV	TGGAGTAAACGGATCGAGTATATG
sHSP23.5_RTPCR_FWD	AACCATCACTCAAACCGACAT
	GGGGACAAGTTTGTACAAAAAAGCAGGCTTCGAAGGAGATAGA
NAC17_Prom1.5KB_GW_FWD	ACTTGAACCATGGTGAATTTGGTG
	GGGGACCACTTTGTACAAGAAAGCTGGGTCTCCACCTCCGGATC
NAC17_Prom1.5KB_GW_FWD	cctacgtaacaaatcaaaaccg
Prom_At3g10500_F	AAAAAGCAGGCTCTCAAGCAGGAACACACAG
Prom_At3g10500_R	AGAAAGCTGGGTCATACTCGATGGACCAAAAC
Prom_At5g04410_F	AAAAAGCAGGCTTATGTATATAGTTAATTTTGCTTAAG
Prom_At5g04410_R	AGAAAGCTGGGTCCAATCGGTGAAAACCAGA
ORF_At3g10500_F	AAAAAGCAGGCTCCACCATGGGTCGTGGCTCAGTAA
ORF_At3g10500_R	AGAAAGCTGGGTCTCACCTGGAAGAGACCAAAATG
ANAC017_FWD	GGGGACAAGTTTGTACAAAAAAGCAGGCTTCATGGCGGATTCTTCACCCGATTCG
ANAC017_REV	GGGGACCACTTTGTACAAGAAAGCTGGGTCCTAGTCTTTCAAGAGAAGACTTC

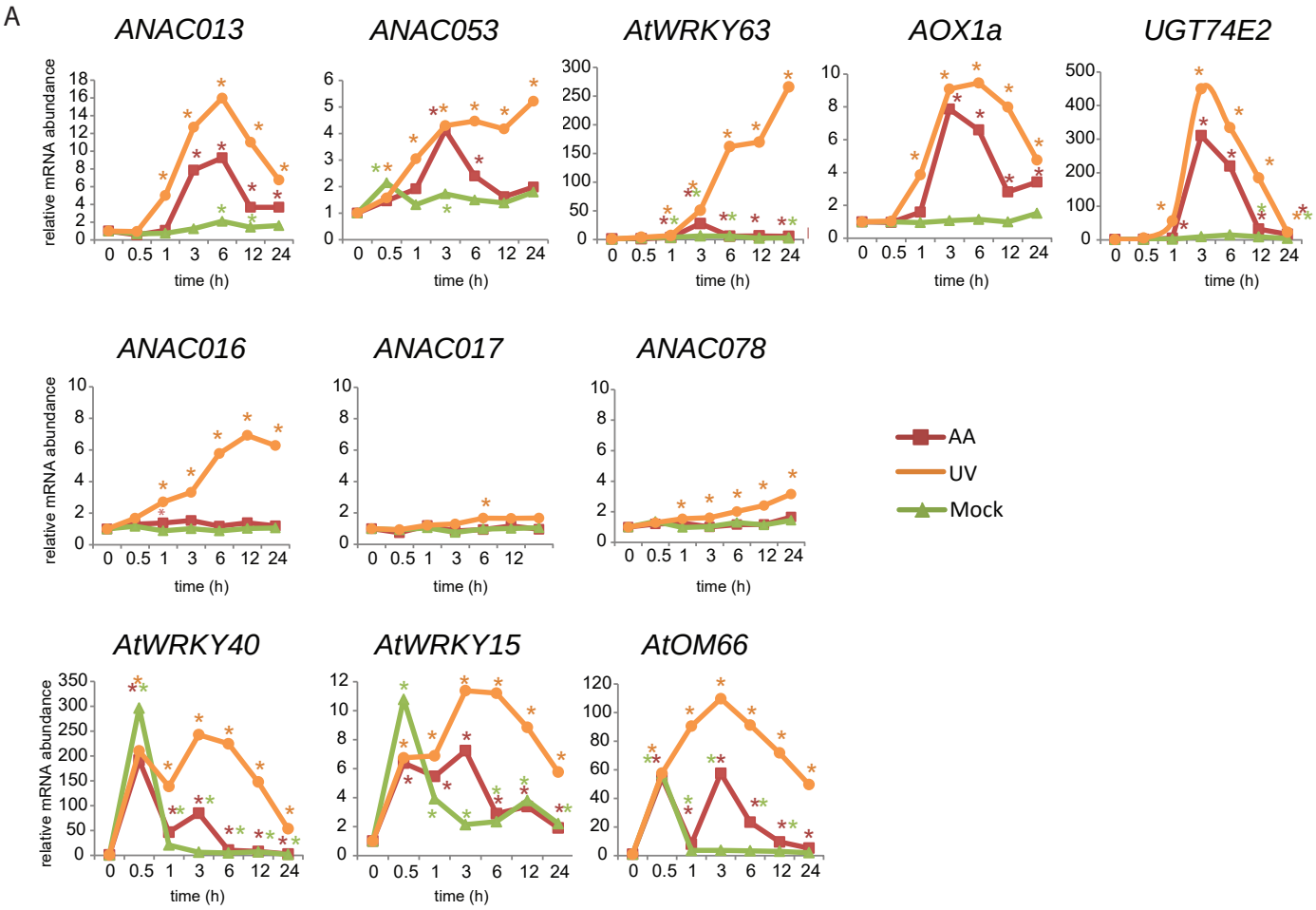

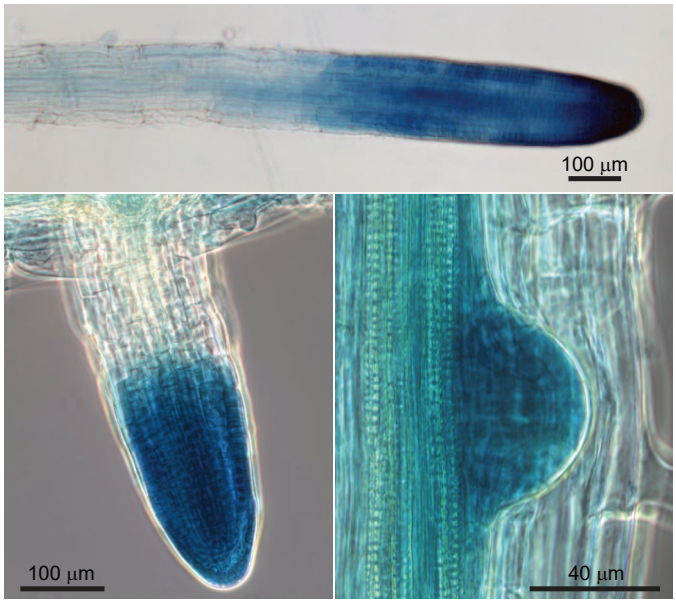

Suppl. Figure 1. UV-induced expression of retrograde-related genes. (A) Two-week old in vitro grown seedlings were exposed to 5 kJ/cm^{2}UV radiation or spray treated with antimycin A or mock solution (water + TWEEN-20). Plants were collected in pools at specified time points and relative mRNA levels of transcription factors and corresponding target genes were measured by qRT-PCR. * $p<0.05$ vs 0h (n=3). All expression values are fold changes normalised to untreated samples (0h). (B) Promoter-GUS analysis of *ANAC017* expression patterns in root tips of 3 week old in vitro grown plants.

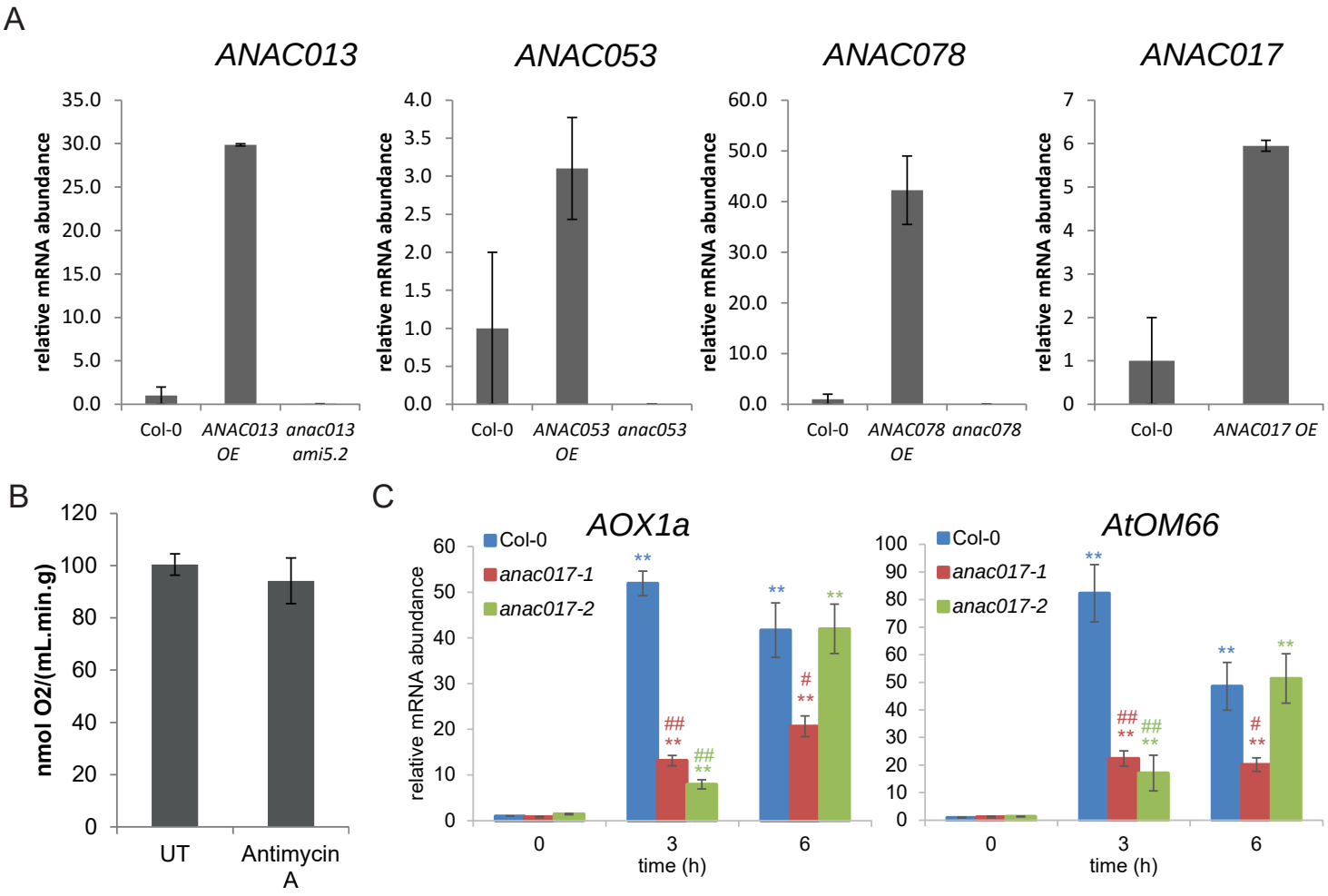

Suppl. Figure 2. (A) Expression levels of target NAC transcription factors in loss- or gain-of-function lines used in this study as determined by qRT-PCR. All values were normalised to Col-0. Error bars indicate standard error. **(B)** 2 week old soil-grown plants were left untreated (UT) or sprayed with 50 μM antimycin A. plants were collected after 4h and dark respiration was measured using a Clark-type oxygen electrode. No statistically significant differences were found between the two conditions ($p>0.50$). **(C)** 2 week old soil-grown plants were sprayed with 50 μM antimycin A. Pools of plants were collected in triplicate at the indicated timepoints and mRNA levels were measured using qRT-PCR and normalised to Col-0 untreated samples (0h). ** indicate statistically significant changes against Col-0 at 0h (** $p<0.01$). #, ## indicate statistically significant changes against Col-0 at the same timepoint. (## $p<0.01$; # $p<0.05$).

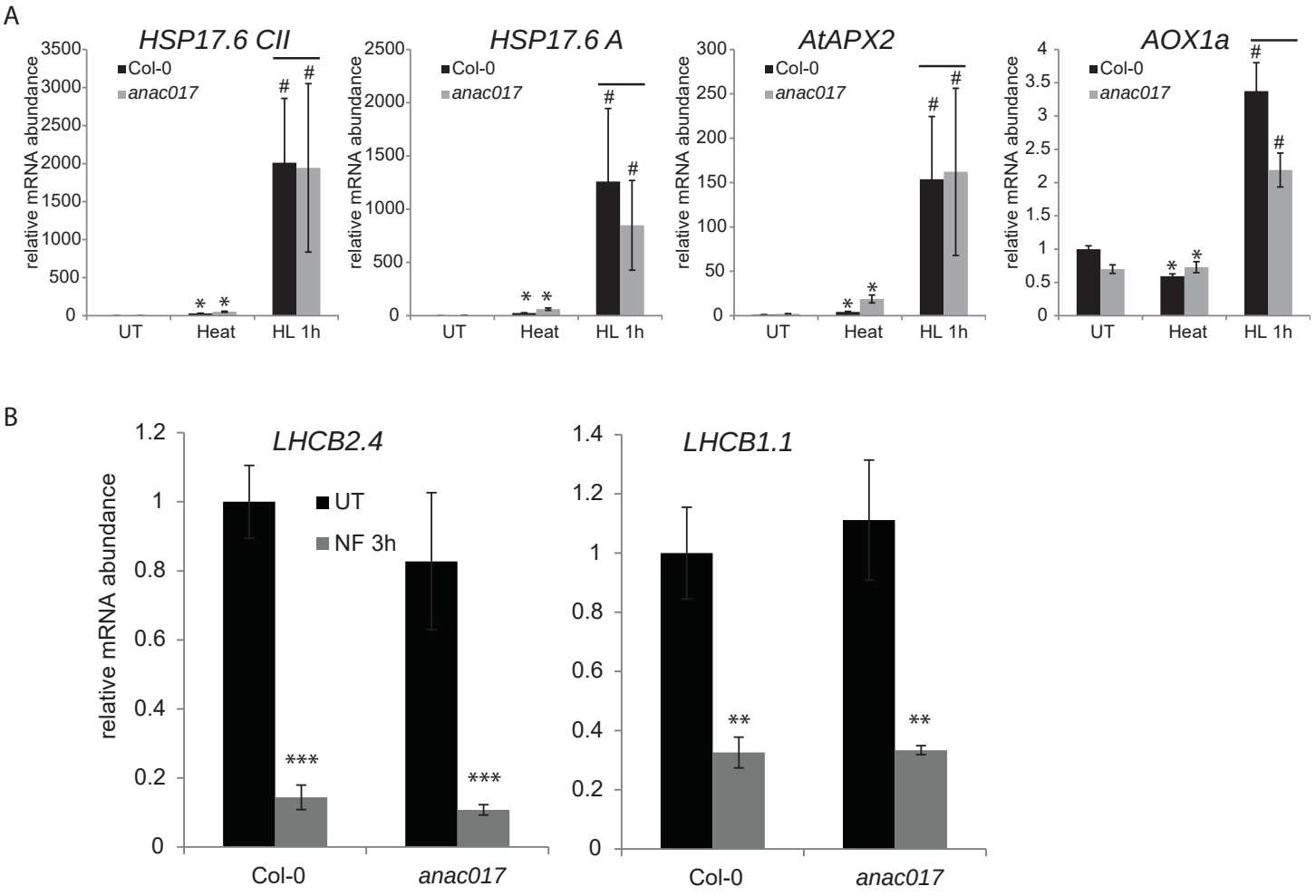

Suppl. Figure 3. ANAC017 is not a regulator of high light- and norflurazon responsive gene expression. Two-week-old *in vitro* grown seedlings of Col-0 and *anac017* plants were treated with (A) 750 µmol s^{-1} m^{-2} of illumination and pooled plants were collected in triplicate (n=3) after 1 h or (B) sprayed with 20 µM norflurazon and pooled plants were collected in triplicate after 3h. Transcript abundance was measured using qRT-PCR and normalised to Col-0 in untreated conditions. Error bars indicate standard error. Statistical test vs Col-0 UT: Student's t-test * p<0.08; ** p<0.05; ***p<0.01; Mann-Whitney U rank-based test: # p<0.05.

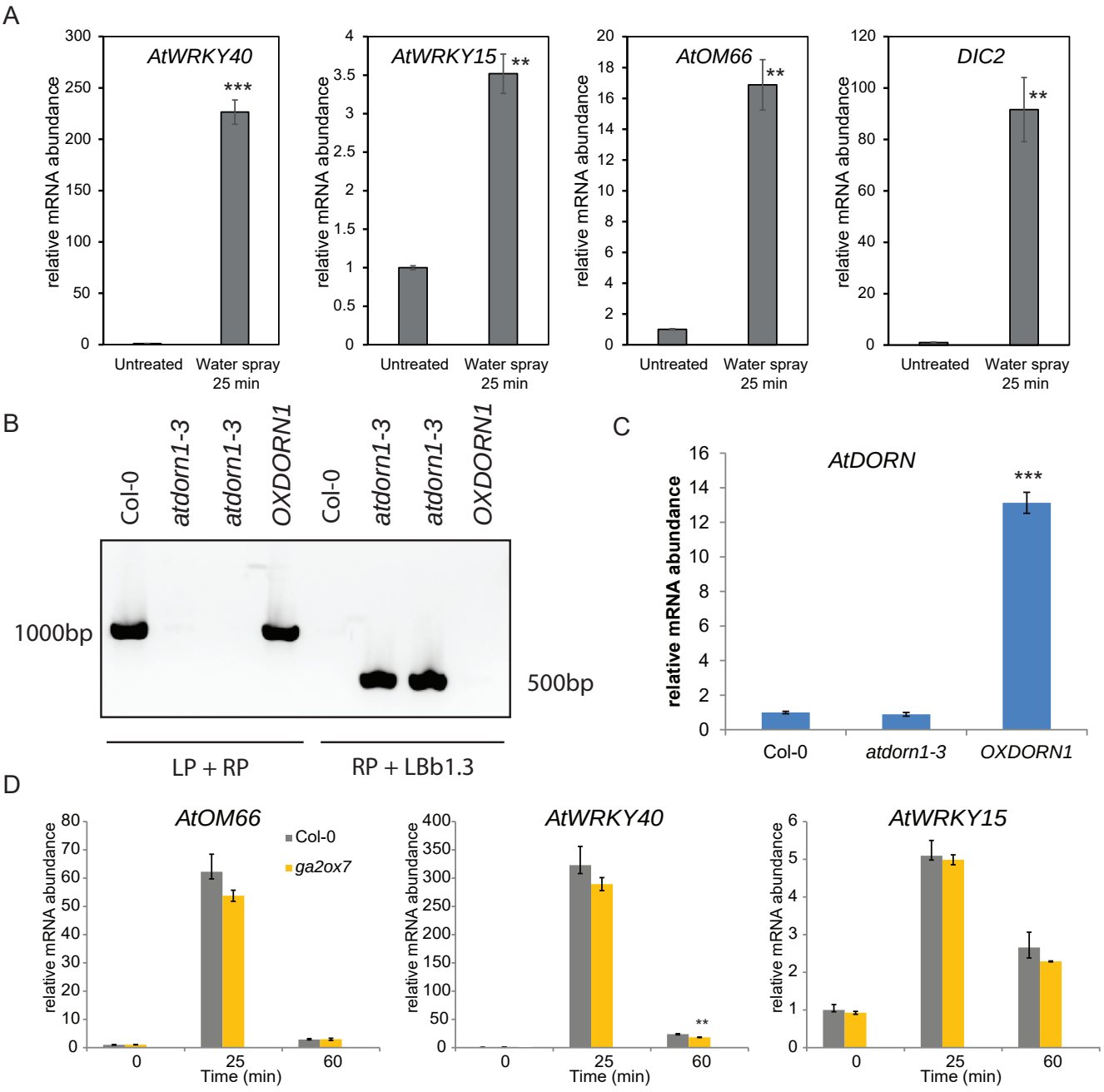

Suppl. Figure 4. Touch responsive gene expression. (A) Pools of in vitro grown seedlings were spray-treated with water and collected in triplicate. mRNA levels were measured using qRT-PCR and normalised to Col-0 untreated. (B) Genotyping of AtDORN1 mutants with left (LP) and right (RP) genomic primers to check presence of WT AtDORN1 alleles, RP and SALK LBb1.3 T-DNA border primer to check presence of T-DNA insertion. (C) QRT-PCR measurement of *AtDORN1* transcript levels in knock-out and overexpression lines. (D) Two-week-old seedlings of different genotypes were spray-treated and pools of plants were collected in triplicate. mRNA levels were measured by qRT-PCR and normalised to Col-0. Statistical significance is indicated by * ($p<0.05$), ** ($p\leq0.01$), *** ($p<0.001$) (n=3).

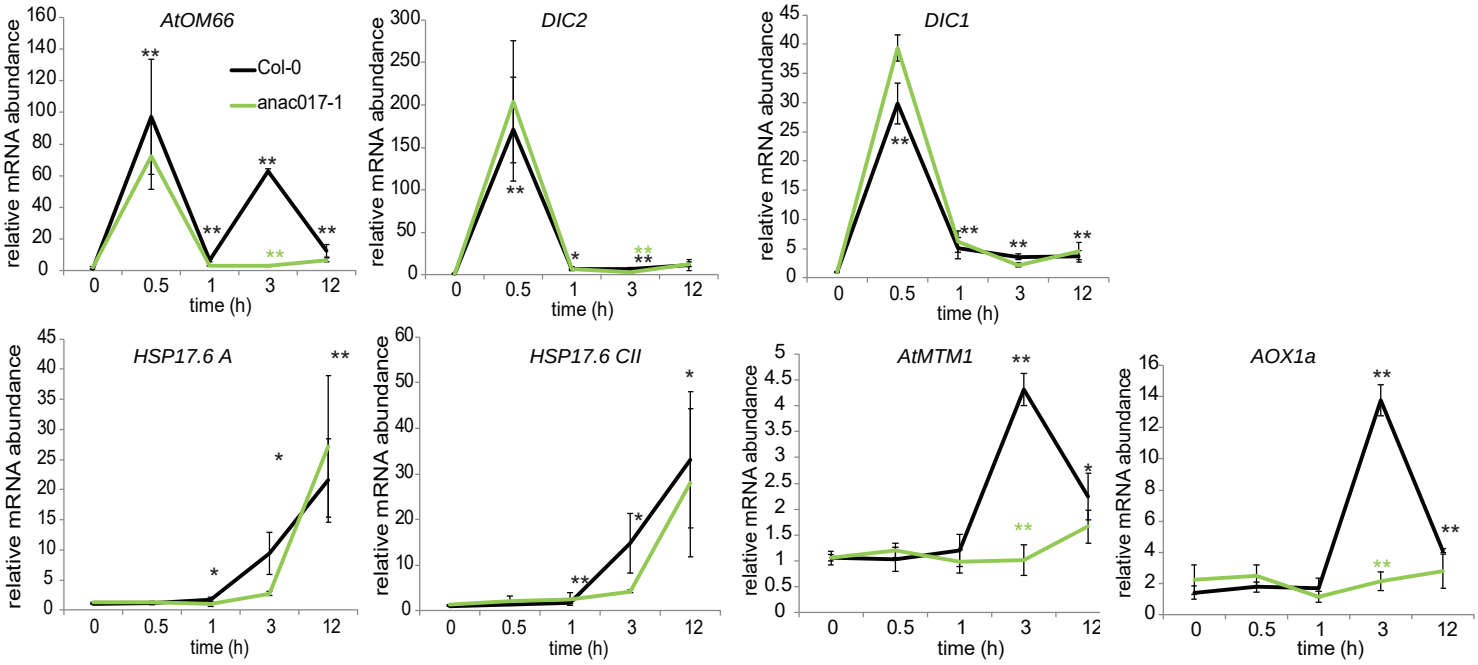

Suppl. Figure 5. Expression patterns of mitochondrial carriers and HSP17.6 during antimycin A treatment. Two-week old *in vitro* grown seedlings of various loss- and gain-of-function lines were spray treated with antimycin A. Plants were collected in pools at specified time points and relative mRNA levels were measured by qRT-PCR . All expression values are fold changes normalised to untreated Col-0 samples (0h). * $p<0.10$; ** $p<0.05$ (n=3)

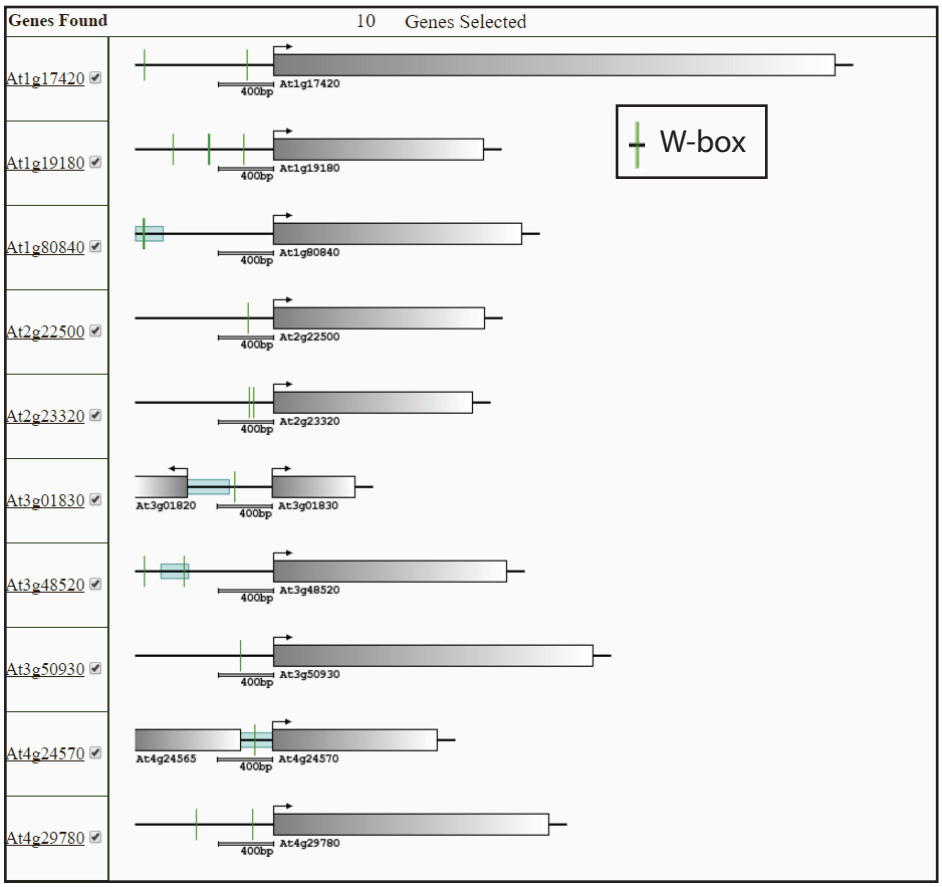

P-value	Name	#P	#S	Select	P-value	Name	#P	#S	Select
#P = Number of promoters with TF sites					#S = Number of predicted TF sites				
0.3473	ABRE binding site motif	1	1		0.5697	ABRE-like binding site motif	2	2	
0.1985	ABREATRD22	1	1		0.3785	ACGTABREMOTIFA2OSEM	2	2	
0.6369	ARF binding site motif	3	5		0.1416	AtMYC2 BS in RD22	5	8	
0.1126	BoxII promoter motif	6	6		0.3977	CACGTGMOTIF	2	4	
0.7147	CARGCW8GAT	5	12		0.4684	CArG promoter motif	1	2	
0.7212	CCA1 binding site motif	2	2		0.2467	CDA1ATCAB2	1	1	
0.8700	DRE core motif	1	1		0.1635	E2F binding site motif	1	1	
0.4781	EveningElement promoter moti	1	1		0.5630	GAREAT	5	8	
0.5966	Gap-box Motif	1	1		0.6857	Ibox promoter motif	3	3	
0.7569	L1-box promoter motif	1	1		0.7481	MYB binding site promoter	2	2	
0.7465	MYB1AT	7	18		0.4366	MYB1LEPR	2	2	
0.7230	MYB2AT	2	2		0.4873	MYB4 binding site motif	7	12	
0.1416	MYCATERD1	5	8		0.2493	RY-repeat promoter motif	1	2	
0.4672	SV40 core promoter motif	2	2		0.1135	T-box promoter motif	7	11	
0.5412	TATA-box Motif	8	25		0.2040	TELO-box promoter motif	2	2	
0.0043	W-box promoter motif	10	18		0.0200	Z-box promoter motif	2	3	

Suppl. Figure 6. Promoter analysis of touch responsive genes. The 1 kb upstream promoter regions of 10 touch responsive genes were analysed by Athena (O'Connor et al., 2005). The top image represents locations in the promoter regions of statistically overrepresented W-box WRKY-binding sites. The table below shows the occurrence of all analysed promoter elements with respective p-values.